arXiv:1304.6644v1 [hep-ph] 24 Apr 2013

Quark sector of S_3 models: classification and comparison with experimental data

F. González Canales[a,b], A. Mondragón[a], M. Mondragón[a], U. J. Saldaña Salazar[a],
and L. Velasco-Sevilla[a,c]

(a) Instituto de Física, Universidad Nacional Autónoma de México,
Apdo. Postal 20-364, 01000, México D.F., México.

(b) Facultad de Ciencias de la Electrónica, Benemérita Universidad Autónoma de Puebla,
Apdo. Postal 157, 72570, Puebla, Pue., México.

(c) University of Hamburg, II. Institute for Theoretical Physics,
Luruper Chaussee 149, 22761 Hamburg, Germany

April 25, 2013

Abstract

S_3 models offer a low energy approach to describe the observed pattern of masses and mixing, of both quarks and leptons. In this work, we first revisit an S_3 model with only one Higgs electroweak doublet, where the flavour symmetry must be broken in order to produce an acceptable pattern of masses and mixing for fermions. Then, we analyse different S_3 models, where the flavour symmetry is preserved as an exact, but hidden symmetry of the low energy spectra, after the electroweak symmetry breaking. The latter models require the addition of two more Higgs electroweak doublets which are accommodated in an S_3 doublet. We also explore the consequences of adding a fourth Higgs electroweak doublet, thus occupying all three irreducible representations of S_3. We show how the various S_3-invariant mass matrices of the different models can reproduce the two texture zeroes and Nearest Neighbour Interaction matrix forms, which have been found to provide a viable and universal treatment of mixing for both quarks and leptons. We also find analytical and exact expressions for the CKM matrix of the models in terms of quark mass ratios. Finally, we compare the expressions of the CKM matrix of the different S_3 models with the most up to date values of masses and mixing in the quark sector, via a χ^2 analysis. We find that the analytical expressions we derived reproduce remarkably well the most recent experimental data of the CKM matrix, suggesting that S_3 is a symmetry of the quark sector.

1 Introduction

The Standard Model (SM) has successfully described the fundamental interactions of elementary particles. It has nineteen free parameters, most of which belong to the masses of fermions and their mixing. Additionally, the introduction of more parameters becomes necessary when the massive nature of neutrinos is considered.

The observed mass spectrum, the mixing pattern, the fact that there appear to be only three generations of matter, the origin of Charge-Parity (CP) violation, among other puzzles, lack an explanation within the theory, and are generically known as the flavour and CP problems respectively (see for example [1, 2]).

The common approach in attempts to solve the flavour puzzle, was by the addition of a horizontal symmetry acting on family space in a non-trivial fashion. The symmetry group which relates families in a non-trivial way is known as the family or flavour symmetry group. On the other hand, it was also noticed that without adding a family symmetry, one can introduce texture zeroes in different positions of the mass matrices to obtain concise relations between mixing angles and mass ratios (see refs. [1, 3–6] for recent reviews). In the late nineteen sixties [7, 8] a relation between the Cabibbo angle and a quark mass ratio, $\theta_{12}^{q} \approx \sqrt{m_d/m_s}$, was found. Then, in the seventies, in a series of papers [9–15], the importance of this relation was realised and generalised in order to relate other mixing angles to mass ratios. We, as other authors, combine both approaches as a stepping stone to find analytical expressions for the mixing angles as functions of the mass ratios.

The introduction to the SM of a non-Abelian discrete family symmetry is the simplest way to relate families non-trivially. The smallest group among these symmetries is the permutational symmetry of three objects, S_3. We remind the reader that there are basically two types of models based on the group S_3. First, there are those models which have only one Higgs field which is a doublet under $SU(2)_L$ and a singlet under S_3 [16–27]. In these models the S_3 flavour symmetry must be broken in order to produce an acceptable pattern of mixing for fermions. Second, there are the class of S_3-invariant models in which the S_3 symmetry is preserved as an exact but hidden symmetry of the low energy spectra after the electroweak symmetry breaking [28–51]. The latter models require the addition of at least two electroweak doublet Higgs fields, besides the Higgs field of the SM. Of these three $SU(2)_L$ doublets, two of them are assigned to the doublet irreducible representation (irrep) of S_3, and the third one is assigned to the singlet one. It is also possible to add extra Abelian discrete symmetries, Z_n, to further reduce the number of parameters.

In the last decade and the first years of the present decade, the experimental knowledge about the magnitudes of all nine elements of the Cabibbo-Kobayashi-Maskawa (CKM) quark mixing matrix, as well as the Jarlskog rephasing invariant, have had a remarkable improvement in precision and quality [52]. At the same time, we have witnessed a spectacular improvement in the determination of mixing and squared mass differences in the neutrino sector [53, 54]. At present, it is crucial for the success of a model of quark and lepton mixing to either agree with the experimental information with great accuracy or, better, to predict accurately the observed mixing and mass patterns.

Here, we build various S_3 models based on the two aforementioned types, *i.e.*, a model with the SM Higgs as an S_3 singlet and models with a total of three or four Higgs $SU(2)_L$ doublets assigned to different irreducible representations of S_3. We then compare the quark sector of the models with the most up to date data on quark masses and mixing. Since S_3 models do not offer an explanation of the value of the quark masses, in order to confront the theoretical form of the CKM mixing with the experimental data, we need to perform a χ^2 fit, where the observables should be four independent parameters of the CKM matrix, and the parameters to be adjusted should be the quark mass ratios and one free parameter for each type of quarks (up and down). The mass ratios are not treated as free parameters, since we allow their values to vary within the three sigma region given by the best fit to experimental data measurements as given in the PDG [52, 55], and our computation at M_Z.

We find a remarkable good quality of the χ^2 fits for the different models in the allowed parameter space of each model. This will make it possible to discriminate among different models when measurements in the quark sector further improve.

In a follow up work [56], we will confront the corresponding masses and mixing of the leptonic sector of each model with the most up to date experimental data. It is important to mention that our approach is at low energies, hence making no assumption of an ultraviolet completion of the theory. However, some of these scenarios can be embedded in Grand Unified Theories (see for instance refs. [57–60]).

The present work is organised as follows. In Sections 2-4, we present the basic ingredients of the S_3 models that we confront with the experimental data on quark masses and mixing. In Section 5, we present the form of the quark mass matrices and relate them to two texture zeroes or Nearest Neighbour Interaction (NNI) mass matrices. In this way, we are able to derive explicit analytical expressions for the elements of the CKM mixing matrix in terms of the quark mass ratios and a few free parameters. In Section 6, we present the prediction of the CKM matrix for each model. In Section 7, we present a detailed χ^2 analysis of the CKM matrix elements and comment on the very good quality of the fit of our models to the most recent experimental data. We conclude in Section 8 with some remarks and an outlook of the present work.

2 S_3 as a family symmetry group

S_3 is the symmetry group of permutations of three objects, which can be geometrically represented by the different rotations that leave invariant an equilateral triangle. It has six elements, the smallest number of elements in non-Abelian discrete groups. It has three irreducible representations (irreps): a doublet $\mathbf{2}$, and two singlets, $\mathbf{1}_S$ and $\mathbf{1}_A$, symmetric and anti-symmetric, respectively. The Kronecker products of the irreps are: $\mathbf{1}_S \otimes \mathbf{1}_S = \mathbf{1}_S$, $\mathbf{1}_A \otimes \mathbf{1}_A = \mathbf{1}_S$,

$\mathbf{1}_A \otimes \mathbf{1}_S = \mathbf{1}_A$, $\mathbf{1}_S \otimes \mathbf{2} = \mathbf{2}$, $\mathbf{1}_A \otimes \mathbf{2} = \mathbf{2}$, and $\mathbf{2} \otimes \mathbf{2} = \mathbf{1}_A \oplus \mathbf{1}_S \oplus \mathbf{2}$.

The only non-trivial tensor product is that of two doublets, $\mathbf{p}_D^T = (p_{D1}, p_{D2})$ and $\mathbf{q}_D^T = (q_{D1}, q_{D2})$, which contains two singlets, $\mathbf{r}_S$ and $\mathbf{r}_A$, and one doublet, $\mathbf{r}_D^T = (r_{D1}, r_{D2})$, where

$$\begin{gathered}\mathbf{r}_S = p_{D1}q_{D1} + p_{D2}q_{D2}, \quad \mathbf{r}_A = p_{D1}q_{D2} - p_{D2}q_{D1}, \\ \mathbf{r}_D^T = (r_{D1}, r_{D2}) = (p_{D1}q_{D2} + p_{D2}q_{D1}, p_{D1}q_{D1} - p_{D2}q_{D2}).\end{gathered}$$

So far, the experimental evidence points to the existence of only three generations of quarks and leptons [61], and we will work under this assumption. The SM Lagrangian makes no distinction between the different families when no Yukawa interactions are present. We take this as a theoretical suggestion of the possible family symmetry relating the three generations of matter. In the following section we will discuss first the matter content and then the Higgs field content of the different models presented here.

3 Matter content of S_3

For fermions, when we choose a three dimensional representation of the group S_3, according to the dimension of the fermion mass matrices, we are led to consider two different direct irreducible decompositions: $3_S \equiv \mathbf{2} \oplus \mathbf{1}_S$, or, $3_A \equiv \mathbf{2} \oplus \mathbf{1}_A$. Then, the assignment of quark families to the irreducible S_3 representations is suggested by the observed mass hierarchy in each fermion sector

$$\begin{aligned}&m_u : m_c : m_t \approx 10^{-6} : 10^{-3} : 1, \quad m_d : m_s : m_b \approx 10^{-4} : 10^{-2} : 1, \\ &m_e : m_\mu : m_\tau \approx 10^{-5} : 10^{-2} : 1. \end{aligned} \tag{1}$$

Hence, we generically assign the first two families, $f_{I(L,R)}$ and $f_{II(L,R)}$, to the doublet representation, $\mathbf{2}$. Then, the third family, $f_{III(L,R)}$, can be chosen to transform as a symmetric singlet representation, $\mathbf{1_S}$ [51], or as an anti-symmetric singlet representation, $\mathbf{1_A}$ [34, 62]. Here we consider the two possibilities and compare the differences that arise among them. The fermions in the doublet representation are denoted by

$$\begin{pmatrix} f_{I(L,R)} \\ f_{II(L,R)} \end{pmatrix} \sim \mathbf{2}, \tag{2}$$

where I, II or III represent the family index of a left- or right-handed fermionic field, $f_{(L)}$ or $f_{(R)}$, respectively. Specifically for quarks we have

$$\begin{aligned}&f_{IIIL} = (b_L, t_L)\ , \quad f_{IIIR} = t_R, \text{ or } f_{IIIR} = b_R \\ &\begin{pmatrix} f_{IL} \\ f_{IIL} \end{pmatrix} = \begin{pmatrix} (u_L, d_L) \\ (c_L, s_L) \end{pmatrix}, \quad \begin{pmatrix} f_{IR} \\ f_{IIR} \end{pmatrix}_{f=u} = \begin{pmatrix} u_R \\ c_R \end{pmatrix}, \quad \begin{pmatrix} f_{IR} \\ f_{IIR} \end{pmatrix}_{f=d} = \begin{pmatrix} d_R \\ s_R \end{pmatrix},\end{aligned} \tag{3}$$

in these expressions, (u_L, d_L) and (c_L, s_L) are doublets under $SU(2)_L$, while u_R, c_R, d_R, and s_R are $SU(2)_L$ singlets.

4 Higgs field content

A state compatible with a SM-like Higgs boson has recently been observed at the LHC [63–65]. We do not have yet any experimental information about the scalar sector of the SM at higher energies, thus it is natural to ponder what are the consequences of having more than one Higgs doublet in extensions of the SM (without SUSY). We thus explore here various scenarios with different numbers of Higgs $SU(2)_L$ doublets.

There are many possibilities to form S_3 invariant scalars with the fermions in the S_3 representations of Eq. (3) and the Higgs fields assigned as

$$H_{DW} \equiv \begin{pmatrix} H_{1W} \\ H_{2W} \end{pmatrix} \sim \mathbf{2}; \quad H_{SW} \sim 1_{\mathbf{S}}; \quad H_{AW} \sim 1_{\mathbf{A}}. \tag{4}$$

The cases we consider are the following:

I. The SM with addition of an S_3 family symmetry, where a single Higgs $SU(2)_L$ doublet is a singlet under S_3. This model can only explain fermion masses and mixing angles when the S_3 symmetry is broken [16, 17, 22].

II. An S_3-invariant extension of the SM with three Higgs $SU(2)_L$ doublets, either as H_{DW} and H_{SW} or as H_{DW} and H_{AW}. The choice of the symmetric or anti-symmetric singlet depends on the resulting form of the mass matrices we want to generate. Here we consider only the invariant scalars that lead to forms of the mass matrices that are able to reproduce the measured values of the CKM matrix, namely the Fritzsch two zeroes texture form, and the Nearest Neighbour Interaction (NNI) one.

III. An S_3-invariant extension of the SM with four Higgs $SU(2)_L$ doublets, which are assigned to all three irreducible representations of S_3: H_{DW}, H_{SW}, and H_{AW}.

In the following section we discuss the cases II and III. The general discussion of the case I can be found in ref. [22], here we present its general features.

5 Mass matrices

5.1 Model with one Higgs doublet

This model has been thoroughly studied in the literature [16,22,66], for completeness, we briefly present it here to compare it with the other models analysed in this work. In this case, the Higgs boson of the SM is an $SU(2)_L$ doublet and, since it has no flavour, it is in a singlet representation of S_3. When S_3 is an exact symmety and the field in the S_3 singlet representation is assigned to the fields in the third generation, then, in a symmetry adapted basis, all elements in the mass matrices should vanish except for the element (3,3). Hence, from the structure of the mass matrices, only the fermion that is assigned to the singlet representation of S_3 acquires mass, and the symmetry should be broken in order to give mass to the other families. Realistic Dirac fermion mass matrices could result from the flavour permutational symmetry $S_{3L} \otimes S_{3R}$ and its spontaneous or explicit breaking according to the chain: $S_{3L} \otimes S_{3R} \supset S_3^{\rm diag} \supset S_{2L} \otimes S_{2R} \supset S_2^{\rm diag}$ [16, 17].

Under an exact $S_{3L} \otimes S_{3R}$ symmetry, the mass spectrum for either the quark sector (up or down quarks) or the leptonic sector (charged leptons or Dirac neutrinos) consists of one massive particle in a singlet irreducible representation and a pair of massless particles in a doublet irreducible representation of $S_{3L} \otimes S_{3R}$. Thus, in the *electroweak basis*, the corresponding mass matrices, $\mathbf{M}_{i3}^{(W)}$, are invariant with respect to a permutation of the family (columns) and flavour (rows) indices, and all entries in $\mathbf{M}_{i3}^{(W)}$ are equal, see Eq. (2.4) in [16]. Once an explicit assignment of particles to the irreducible representations of S_3 is made, it is convenient to make a change of basis from the electroweak basis to a *symmetry adapted* or *hiererchical basis* by means of the unitary matrix that diagonalises the matrix $\mathbf{M}_{i3}^{(W)}$,

$$\mathbf{M}_{i3}^{(H)} = \mathbf{U}^{\dagger} \mathbf{M}_{i3}^{(W)} \mathbf{U}, \tag{5}$$

where

$$\mathbf{U} = \frac{1}{\sqrt{6}} \begin{pmatrix} \sqrt{3} & 1 & \sqrt{2} \\ -\sqrt{3} & 1 & \sqrt{2} \\ 0 & -2 & \sqrt{2} \end{pmatrix} \quad \text{and} \quad \mathbf{M}_{i3}^{(H)} = m_{i3} \begin{pmatrix} 0 & 0 & 0 \\ 0 & 0 & 0 \\ 0 & 0 & 1-\Delta_i \end{pmatrix}_H . \tag{6}$$

In the electroweak basis the masses for the first two families are generated by introducing the terms,

$$\mathbf{M}_{i2}^{(W)} = \frac{m_{i3}}{3} \begin{pmatrix} \alpha_i & \alpha_i & \beta_i \\ \alpha_i & \alpha_i & \beta_i \\ \beta_i & \beta_i & -2\beta_i \end{pmatrix}_W \quad \text{and} \quad \mathbf{M}_{i1}^{(W)} = \frac{m_{i3}}{\sqrt{3}} \begin{pmatrix} A_{i1} & iA_{i2} & -A_{i1} - iA_{i2} \\ -iA_{i2} & -A_{i1} & -A_{i1} + iA_{i2} \\ -A_{i1} - iA_{i2} & A_{i1} - iA_{i2} & 0 \end{pmatrix}_W . \tag{7}$$

In the matrix $\mathbf{M}_{i2}$, α_i and β_i are real numbers that parametrize the most general form of a matrix invariant under the permutations of the first two columns or rows. In $\mathbf{M}_{i1}$, A_{i1} and A_{i2} are also real parameters, through which it is possible to construct a complex representation of $S_3^{\rm diag}$, that allows us to have a CP-violating phase in the mixing matrix [16]. The term $\mathbf{M}_{i2}^{(W)}$ breaks the permutational symmetry $S_{3L} \otimes S_{3R}$ down to $S_{2L} \otimes S_{2R}$ and mixes the singlet and doublet representations of S_3, while the term $\mathbf{M}_{i1}^{(W)}$ transforms as the mixed symmetry term of the doublet complex tensorial representation of the $S_3^{\rm diag}$ diagonal subgroup of $S_{3L} \otimes S_{3R}$. Thus, taking into account all the terms of Eqs. (5)-(7), the mass matrix $\mathbf{M}_i^{(H)}$ in a symmetry adapted basis takes the form

$$\mathbf{M}_i^{(H)} = m_{i3} \begin{pmatrix} 0 & A_i & 0 \\ A_i^* & B_i & C_i \\ 0 & C_i & D_i \end{pmatrix}_H , \qquad i = u, d, l, \nu_D, \tag{8}$$

where $A_i = |A_i|e^{i\phi_i}$, $B_i = -\triangle_i + \delta_i$, and $D_i = 1 - \delta_i$. From the strong hierarchy of the masses of the Dirac fermions, $m_{i3} >> m_{i2} > m_{i1}$, we expect $1 - \delta_i$ to be very close to unity.

5.2 Models with three or four Higgs fields

After the electroweak symmetry breaking, the Higgs $SU(2)_L$ doublets acquire real vacuum expectation values (vev's),

$$w_1 \equiv \langle 0|H_{1W}|0\rangle, \;\; w_2 \equiv \langle 0|H_{2W}|0\rangle, \;\; v_S \equiv \langle 0|H_{SW}|0\rangle, \;\; \text{and} \;\; v_A \equiv \langle 0|H_{AW}|0\rangle, \tag{9}$$

giving masses to all fermions of the SM. The notation we use for the effective mass Lagrangian of these models is

$$\mathcal{L}_q = -\frac{1}{2}(\bar{u}_L, \bar{c}_L, \bar{t}_L)\mathcal{M}^u_{S_3}\begin{pmatrix} u_R \\ c_R \\ t_R \end{pmatrix} - \frac{1}{2}(\bar{d}_L, \bar{s}_L, \bar{b}_L)\mathcal{M}^d_{S_3}\begin{pmatrix} d_R \\ s_R \\ b_R \end{pmatrix} + h.c.. \tag{10}$$

In order to make the analysis as general as possible, we first write all possible Yukawa interactions which arise with the matter and Higgs content of Eqs. (3) and (4) when assigning the third family to different representations.

Third family in the symmetric singlet representation: For this case, both f_{IIIL} and f_{IIIR} transform as $\mathbf{1_S}$

$$\begin{aligned} -\mathcal{L}_{Y_f} = {} & Y_1^f\left(\overline{f}_{IIIL}f_{IIIR}H_{SW}\right) + \frac{1}{\sqrt{2}}Y_2^f(\overline{f}_{1W}f_{1R} + \overline{f}_{2W}f_{2R})H_{SW} + \\ & \frac{1}{2}Y_3^f\left[(\overline{f}_{1W}H_{2W} + \overline{f}_{2W}H_{1W})f_{1R} + (\overline{f}_{1W}H_{1W} - \overline{f}_{2W}H_{2W})f_{2R}\right] + \\ & \frac{1}{\sqrt{2}}Y_4^f(\overline{f}_{1W}f_{2R} - \overline{f}_{2W}f_{1R})H_{AW} + \frac{1}{\sqrt{2}}Y_5^f(\overline{f}_{1W}H_{1W} + \overline{f}_{2W}H_{2W})f_{IIIR} + \\ & \frac{1}{\sqrt{2}}Y_6^f\left[\overline{f}_{IIIL}(H_{1W}f_{1R} + H_{2W}f_{2R})\right] + h.c., \quad f = d,\ e, \end{aligned} \tag{11}$$

where Y_j^f, with $j = 1\cdots 6$, are complex Yukawa couplings. When writing the Yukawa Lagrangian, for up quarks or Dirac neutrinos, the Higgs fields should be replaced by the respective conjugate Higgs fields, $H_{iW} \to i\sigma_2 H^*_{iW}$, $i = 1, 2$. After the electroweak symmetry breaking, both up and down quark mass matrices take the generic form

$$\mathcal{M}^f_{S_3} = \begin{pmatrix} \sqrt{2}Y_2^f v_S + Y_3^f w_2 & Y_3^f w_1 + \sqrt{2}Y_4^f v_A & \sqrt{2}Y_5^f w_1 \\ Y_3^f w_1 - \sqrt{2}Y_4^f v_A & \sqrt{2}Y_2^f v_S - Y_3^f w_2 & \sqrt{2}Y_5^f w_2 \\ \sqrt{2}Y_6^f w_1 & \sqrt{2}Y_6^f w_2 & 2Y_1^f v_S \end{pmatrix}, \tag{12}$$

whose eigenvalues will be denoted as m_i, $i = 1, 2, 3$.

Third family in the anti-symmetric representation: In this case, both f_{IIIL} and f_{IIIR} transform as $\mathbf{1_A}$

$$\begin{aligned} -\mathcal{L}_{Y_f} = {} & Y_1^f \left(\overline{f}_{IIIL} f_{IIIR} H_{SW}\right) + \frac{1}{\sqrt{2}} Y_2^f (\overline{f}_{1W} f_{1R} + \overline{f}_{2W} f_{2R}) H_{SW} + \\ & \frac{1}{2} Y_3^f \left[(\overline{f}_{1W} H_{2W} + \overline{f}_{2W} H_{1W}) f_{1R} + (\overline{f}_{1W} H_{1W} - \overline{f}_{2W} H_{2W}) f_{2R}\right] + \\ & \frac{1}{\sqrt{2}} Y_4^f (\overline{f}_{1W} f_{2R} - \overline{f}_{2W} f_{1R}) H_{AW} + \frac{1}{\sqrt{2}} Y_5^f (\overline{f}_{1W} H_{2W} - \overline{f}_{2W} H_{1W}) f_{IIIR} + \\ & \frac{1}{\sqrt{2}} Y_6^f \left[\overline{f}_{IIIL} (H_{1W} f_{2R} - H_{2W} f_{1R})\right] + h.c., \quad f = d,\ e. \end{aligned} \tag{13}$$

Third family in mixed representations: f_{IIIL} transforming as $\mathbf{1_A}$ and f_{IIIR} transforming as $\mathbf{1_S}$

$$\begin{aligned} -\mathcal{L}_{Y_f} = {} & Y_1^f \left(\overline{f}_{IIIL} f_{IIIR} H_{AW}\right) + \frac{1}{\sqrt{2}} Y_2^f (\overline{f}_{1W} f_{1R} + \overline{f}_{2W} f_{2R}) H_{SW} + \\ & \frac{1}{2} Y_3^f \left[(\overline{f}_{1W} H_{2W} + \overline{f}_{2W} H_{1W}) f_{1R} + (\overline{f}_{1W} H_{1W} - \overline{f}_{2W} H_{2W}) f_{2R}\right] + \\ & \frac{1}{\sqrt{2}} Y_4^f (\overline{f}_{1W} f_{2R} - \overline{f}_{2W} f_{1R}) H_{AW} + \frac{1}{\sqrt{2}} Y_5^f (\overline{f}_{1W} H_{1W} + \overline{f}_{2W} H_{2W}) f_{IIIR} + \\ & \frac{1}{\sqrt{2}} Y_6^f \left[\overline{f}_{IIIL} (H_{1W} f_{2R} - H_{2W} f_{1R})\right] + h.c., \quad f = d,\ e\ , \end{aligned} \tag{14}$$

and f_{IIIL} transforming as $\mathbf{1_S}$ and f_{IIIR} transforming as $\mathbf{1_A}$

$$\begin{aligned} -\mathcal{L}_{Y_f} = {} & Y_1^f \left(\overline{f}_{IIIL} f_{IIIR} H_{AW}\right) + \frac{1}{\sqrt{2}} Y_2^f (\overline{f}_{1W} f_{1R} + \overline{f}_{2W} f_{2R}) H_{SW} + \\ & \frac{1}{2} Y_3^f \left[(\overline{f}_{1W} H_{2W} + \overline{f}_{2W} H_{1W}) f_{1R} + (\overline{f}_{1W} H_{1W} - \overline{f}_{2W} H_{2W}) f_{2R}\right] + \\ & \frac{1}{\sqrt{2}} Y_4^f (\overline{f}_{1W} f_{2R} - \overline{f}_{2W} f_{1R}) H_{AW} + \frac{1}{\sqrt{2}} Y_5^f (\overline{f}_{1W} H_{2W} - \overline{f}_{2W} H_{1W}) f_{IIIR} + \\ & \frac{1}{\sqrt{2}} Y_6^f \left[\overline{f}_{IIIL} (H_{1W} f_{1R} + H_{2W} f_{2R})\right] + h.c., \quad f = d,\ e. \end{aligned} \tag{15}$$

We define the notation

$$\begin{array}{lll} \mu_1^f \equiv \sqrt{2} Y_2^f v_S, & \mu_2^f \equiv Y_3^f w_2, & \mu_3^f \equiv 2 Y_1^f v_S, \\ \mu_4^f \equiv Y_3^f w_1, & \mu_5^f \equiv \sqrt{2} Y_4^f v_A, & \mu_6^f \equiv \sqrt{2} Y_5^f w_1, \\ \mu_7^f \equiv \sqrt{2} Y_5^f w_2, & \mu_8^f \equiv \sqrt{2} Y_6^f w_1, & \mu_9^f \equiv \sqrt{2} Y_6^f w_2, \\ \nu_3^f \equiv 2 Y_1^f v_A, & & \end{array} \tag{16}$$

which will allow us to express the mass matrices in a concise way, focusing on the number of effective parameters entering into each matrix. In the following subsections we present the constraints that we require in order to have a successful description of quark masses and their mixing for each of the above mentioned cases.

5.2.1 Case II: Three Higgs fields

Cases with H_{DW} and H_{SW}. When the left- and the right-handed parts of the third fermion family are assigned to different singlet representations of S_3, symmetric or anti-symmetric, and are coupled to a Higgs field in the singlet symmetric representation of S_3, its Yukawa coupling vanishes. Hence, this possibility is not feasible for a model of fermion masses precisely because the masses of the third fermion family are the largest ones. Due to this fact, if we choose a Higgs field in the singlet symmetric representation of S_3, both left- and right-handed parts of the third family of fermions, $f_{III(L,R)}$, must be chosen to transform either as the symmetric or as the anti-symmetric singlet representation of S_3. We can obtain the form of the mass matrices by taking the limit of $H_{AW} \to 0$ in Eqs. (11)-(13), for the cases of either both left- and right-handed parts of f_{III} in the symmetric, or anti-symmetric singlet representation of S_3, respectively.

The first two cases, A and A', of Tab. 1, corresponds to the case where both the left- and right-handed parts of the third family are in the symmetric singlet representation of S_3, $\mathbf{1}_S$. The cases B and B', correspond to the case where both the left- and right-handed parts of the third family are in the anti-symmetric singlet representation of S_3, $\mathbf{1}_A$. The first column of Tab. 1 denotes the labelling we use, while the third one, gives the form of the mass matrices after the electroweak symmetry breaking (EWSB). Note that for these matrices, the elements $(1,1)$, $(1,3)$, and $(3,1)$ are not different from zero. The fourth column, sub-case A, corresponds to a matrix $\widehat{\mathcal{M}}^f_{Hier}$, where we have rotated the matrix to a basis where the entries $(1,3)$ and $(3,1)$ vanish and we have subtracted the element $\mathcal{M}^f_{Hier}[1,1]$, which will be denoted by μ^f_0, from the diagonal

$$\mathcal{M}^f_{S_3} \longrightarrow \mathcal{M}^f_{Hier} \equiv \mathcal{R}(\theta)_{12} \mathcal{M}^f_{S_3} \mathcal{R}(\theta)^T_{12} = \left(\begin{array}{ccc} \mu^f_0 & a^f & 0 \\ a^{f*} & b^f & c^f \\ 0 & c^{f*} & d^f \end{array} \right) = \mu^f_0 \mathbf{1}_{3\times 3} + \widehat{\mathcal{M}}^f_{Hier} \ , \tag{17}$$

where a^f, b^f, c^f, d^f, and μ^f_0 are shorthand for the entries in the rotated mass matrix $\mathcal{M}^f_{S_3}$. Now, the matrix $\widehat{\mathcal{M}}^f_{Hier}$ has two texture zeroes

$$\widehat{\mathcal{M}}^f_{Hier} = \left(\begin{array}{ccc} 0 & a^f & 0 \\ a^{f*} & b'^f & c^f \\ 0 & c^{f*} & d'^f \end{array} \right) = \left(\begin{array}{ccc} 0 & a^f & 0 \\ a^{f*} & b^f - \mu^f_0 & c^f \\ 0 & c^{f*} & d^f - \mu^f_0 \end{array} \right), \tag{18}$$

and eigenvalues denoted as σ_i^f, $i = 1, 2, 3$. Then, the physical masses m_i^f are related to the shifted masses σ_i^f simply by

$$m_i^f = \mu_0^f + \sigma_i^f. \tag{19}$$

Both transformations, the shift and the rotation, are unobservable in the quark mixing sector, as long as we rotate both matrices, in the u and d sectors, with the same angle θ [1]. The rotation in the right hand side of Eq. (10) is absorbed in the redefinition of the right-handed quarks of Eq. (10).

The vanishing of the entries $(1, 3)$ and $(3, 1)$ in the rotated mass matrix $\mathcal{M}_{Hier}^f$ is only possible if the rotation angle, θ, and the real expectation values of the Higgs fields in the doublet irrep, w_1 and w_2, see Eq.(9), are related by the condition

$$\tan\theta = w_1/w_2. \tag{20}$$

The diagonalising matrices that enter in the definition of the quark mixing matrix, V_{CKM}, may be obtained from the diagonalisation of $\widehat{\mathcal{M}}_{Hier}^f$ instead of $\mathcal{M}_{S_3}^f$. Since there are no right-handed currents in these models, $\widehat{\mathcal{M}}_{Hier}^f$ may be constrained to be Hermitian without any loss of generality [1].

It is interesting to notice that, in order to reproduce the Nearest Neighbour Interaction (NNI) mass matrix form [67, 68], it is enough to fix the rotation angle in Eq. (17) at $\theta = \pi/6$, no Hermiticity of the mass matrix is required. This is also important since the NNI mass matrix form has been shown to provide a good description of the mixing angles in a unified treatment for quarks and leptons [22, 69]. This is the subcase A' in Table 1.

When the third family of fermions is assigned to the anti-symmetric singlet representation of S_3 we obtain fermion mass matrices with two texture zeroes or the equally successful NNI form. These are the cases B and B' in Table 1.

This shows that the requirement of invariance under the S_3 flavour symmetry group generates the phenomenologically successful Fritzsch-like mass matrices with two texture zeroes form and the equally successful NNI form.

Cases with H_{DW} and H_{AW}. As mentioned before, when the left- and right-handed parts of the third generation fermion fields are assigned to the singlet representations of S_3, one to the symmetric and the other to the anti-symmetric one, the Higgs field in the singlet representation of S_3 should be assigned to the anti-symmetric singlet of S_3 to form a non-vanishing Yukawa coupling.

The form of the resulting mass matrices is shown in the third column of Tab. 2. The form that these matrices take after a transformation to a basis where some of its elements are zero is shown in the fourth column of the same Table. The particular cases when the rotation angle is $\pi/6$, denoted as C' and D' correspond to the second and fourth row of Tab. 2.

---

[1] The details of the shift and the rotation are given in Section 5.3 and in the Appendix A.

3HDM: $G_{SM} \otimes S_3$

	$\mathcal{F}_L$	$\mathcal{F}_R$	Mass matrix (FB)	Possible mass textures
A	$\mathbf{2}$, $1_{\mathbf{S}}$	$\mathbf{2}$, $1_{\mathbf{S}}$	$\begin{pmatrix} \mu_1^f + \mu_2^f & \mu_4^f & \mu_6^f \\ \mu_4^f & \mu_1^f - \mu_2^f & \mu_7^f \\ \mu_8^f & \mu_9^f & \mu_3^f \end{pmatrix}$	$\begin{pmatrix} 0 & \mu_2^f sc\,(3-t^2) & 0 \\ \mu_2^f sc\,(3-t^2) & -2\mu_2^f c^2\,(1-3t^2) & \mu_7^f/c \\ 0 & \mu_7^{f*}/c & \mu_3^f - \mu_1^f - \mu_2^f c^2(1-3t^2) \end{pmatrix}$
$A^{'}$				$\begin{pmatrix} 0 & \frac{2}{\sqrt{3}}\mu_2^f & 0 \\ \frac{2}{\sqrt{3}}\mu_2^f & 0 & \frac{2}{\sqrt{3}}\mu_7^f \\ 0 & \frac{2}{\sqrt{3}}\mu_9^f & \mu_3^f - \mu_1^f \end{pmatrix}$
B	$\mathbf{2}$, $1_{\mathbf{A}}$	$\mathbf{2}$, $1_{\mathbf{A}}$	$\begin{pmatrix} \mu_1^f + \mu_2^f & \mu_4^f & \mu_7^f \\ \mu_4^f & \mu_1^f - \mu_2^f & -\mu_6^f \\ -\mu_9^f & \mu_8^f & \mu_3^f \end{pmatrix}$	$\begin{pmatrix} 0 & -\mu_4^f c^2\,(1-3t^2) & 0 \\ -\mu_4^f c^2\,(1-3t^2) & 2\mu_4^f sc\,(3-t^2) & -\mu_6^f/c \\ 0 & -\mu_6^{f*}/c & \mu_3^f - \mu_1^f + \vert\mu_4^f sc(3-t^2) \end{pmatrix}$
$B^{'}$				$\begin{pmatrix} 0 & -2\mu_4^f & 0 \\ -2\mu_4^f & 0 & -2\mu_6^f \\ 0 & 2\mu_8^f & \mu_3^f - \mu_1^f \end{pmatrix}$

Table 1: Mass matrices in S_3 flavour models with three Higgs $SU(2)_L$ doublets: H_{1W} and H_{2W}, which occupy the S_3 reducible representation $\mathbf{2}$, andH_{SW}, which transforms as $1_{\mathbf{S}}$ for the cases when both the left- and right-handed fermion fields are in the same assignment. The mass matrices shown here follow a normal ordering of their mass eigenvalues (m_1^f, m_2^f, m_3^f). We have denoted $s = \sin\theta$, $c = \cos\theta$ and $t = \tan\theta$. The third column of this table corresponds to the general case, while the fourth column to a case where we have rotated the matrix to a basis where the elements $(1,1)$, $(1,3)$ and $(3,1)$ vanish. The primed cases, A' or B', are particular cases of the unprimed ones, A or B, with $\theta = \pi/6$ or $\theta = \pi/3$, respectively.

3HDM: $G_{SM} \otimes S_3$

Name	$\mathcal{F}_L$	$\mathcal{F}_R$	Mass matrix (FB)	Possible mass textures
C	$\mathbf{2}$, $1_{\mathbf{A}}$	$\mathbf{2}$, $1_{\mathbf{S}}$	$\begin{pmatrix} \mu_2^f & \mu_4^f + \mu_5^f & \mu_6^f \\ \mu_4^f - \mu_5^f & -\mu_2^f & \mu_7^f \\ -\mu_9^f & \mu_8^f & \nu_3^f \end{pmatrix}$	$\begin{pmatrix} 0 & A_{12} & 0 \\ A_{21} & A_{22} & A_{23} \\ -A_{32} & 0 & A_{33}(\mu_3^f \to \nu_3^f) \end{pmatrix}$, $\begin{pmatrix} 0 & B_{12} & -B_{23} \\ B_{21} & B_{22} & 0 \\ 0 & B_{32} & B_{33}(\mu_3^f \to \nu_3^f) \end{pmatrix}$
C'				$\begin{pmatrix} 0 & A'_{12} & 0 \\ A'_{21} & 0 & A'_{23} \\ -A'_{32} & 0 & A'_{33}(\mu_3^f \to \nu_3^f) \end{pmatrix}$, $\begin{pmatrix} 0 & B'_{12} & -B'_{23} \\ B'_{21} & 0 & 0 \\ 0 & B'_{32} & B'_{33}(\mu_3^f \to \nu_3^f) \end{pmatrix}$
D	$\mathbf{2}$, $1_{\mathbf{S}}$	$\mathbf{2}$, $1_{\mathbf{A}}$	$\begin{pmatrix} \mu_2^f & \mu_4^f + \mu_5^f & \mu_7^f \\ \mu_4^f - \mu_5^f & -\mu_2^f & -\mu_6^f \\ \mu_8^f & \mu_9^f & \nu_3^f \end{pmatrix}$	$\begin{pmatrix} 0 & A_{12} & A_{23} \\ A_{21} & A_{22} & 0 \\ 0 & A_{32} & A_{33}(\mu_3^f \to \nu_3^f) \end{pmatrix}$, $\begin{pmatrix} 0 & B_{12} & 0 \\ B_{21} & B_{22} & B_{23} \\ B_{32} & 0 & B_{33}(\mu_3^f \to \nu_3^f) \end{pmatrix}$
D'				$\begin{pmatrix} 0 & A'_{12} & A'_{23} \\ A'_{21} & 0 & 0 \\ 0 & A'_{32} & A'_{33}(\mu_3^f \to \nu_3^f) \end{pmatrix}$, $\begin{pmatrix} 0 & B'_{12} & 0 \\ B'_{21} & 0 & B'_{23} \\ B'_{32} & 0 & B'_{33}(\mu_3^f \to \nu_3^f) \end{pmatrix}$

Table 2: Mass matrices in S_3-invariant family models with three Higgs $SU(2)_L$ doublets: H_{1W} and H_{2W} are assigned to the S_3 doublet irreducible representation $\mathbf{2}$, and H_{AW}, transforms as $1_{\mathbf{A}}$. We consider the cases of having the left and right parts of the fermion fields assigned one to the symmetric and the other to the anti-symmetric singlet representations of S_3, since only these combinations give rise to a non-vanishing $(3,3)$ entry in the mass matrix. In all cases it is assumed that the mass eigenvalues follow a normal order in terms of magnitudes. To simplify the notation, X_{ij} denotes the entry (i,j) in X which is any of the mass textures shown in Table 1. The primed matrix elements, A'_{ij} or B'_{ij}, are particular cases of the unprimed ones, A_{ij} or B_{ij}, with $\theta = \pi/6$ or $\theta = \pi/3$, respectively.

5.2.2 Effective number of parameters

Pakvasa and Sugawara [28] analysed for the first time the Higgs potential involving two Higgs fields in the doublet irrep of S_3 and a third one in the symmetric singlet irrep. They found an accidental S_2' symmetry at the minimum if one requires $w_1 = w_2$, which in turn implies the following equalities

$$\mu_2^f = \mu_4^f, \quad \mu_6^f = \mu_7^f, \quad \mu_8^f = \mu_9^f \ , \tag{21}$$

reducing the number of parameters. The corresponding mass matrices thus reduce to the cases of Tab. 3, where we have written down the effective number of free parameters involved in each sector. The form of the matrices of the fourth columns of Tabs. 1-2 is independent of this assumption. Here, by effective free parameters we mean the independent real parameters to be adjusted on a χ^2 analysis. Hence, the counting is performed by considering that each matrix has only a single independent phase plus the number of absolute magnitudes of the complex free parameters. Comparing the number of effective free parameters with the number of real positive parameters in the general case,

$$\mu_1^f,\ \mu_2^f,\ \mu_3^f,\ |\mu_7^f|,\ \theta \text{ and } \arg\left[\mu_7^f\right] , \tag{22}$$

we find they are equal, since in both cases since in both cases the submatrices formed by the elements $(1,1)$, $(1,2)$, $(2,1)$, and $(2,2)$ are parameterized by only two different parameters. Since these parameters are physically irrelevant, we conclude that from the point of view of the quark mass matrices, the assumption $w_1 = w_2$ yields the same result as assuming that w_1 and w_2 are related through Eq. (20). In the cases A(A') and B(B') of Tab. 2 we notice that after reparametrizing the mass matrices in terms of their eigenvalues, the resulting expressions for the entries in the CKM mixing matrix expressed in terms of the quark masses are the same. Therefore, the quark mixing is insensitive to whether the assignment of the third family is done to the symmetric or anti-symmetric singlet. Both cases will lead to the same result.

Name	Mass matrix form	No. of effective real free parameters
A	$\begin{pmatrix} \mu_1^f + \mu_2^f & \mu_2^f & \mu_6^f \\ \mu_2^f & \mu_1^f - \mu_2^f & \mu_6^f \\ \mu_8^f & \mu_8^f & \mu_3^f \end{pmatrix}$	6
B	$\begin{pmatrix} \mu_1^f + \mu_2^f & \mu_2^f & \mu_6^f \\ \mu_2^f & \mu_1^f - \mu_2^f & -\mu_6^f \\ -\mu_8^f & \mu_8^f & \mu_3^f \end{pmatrix}$	6

Table 3: Form of the mass matrices for the cases of Tab. 1 where we have assumed $w_1 = w_2$. This corresponds to the case where the vacuum of the spontaneous symmetry breaking of the EW×S_3 theory has an accidental S_2' symmetry.

5.2.3 Case III: Four Higgs fields

In case III all terms of Eqs. (11), (13-15) should be present. As in the previous subsection, we have identified the transformations that yield (a) a Hermitian matrix with vanishing elements $(1,3)$, $(3,1)$ and $(1,1)$, and (b) a NNI matrix form. Now, taking into account all terms in Eqs. (17, 18), all the possible forms of the mass matrices that we obtain appear in Tab. 4.

5.3 Diagonalisation Procedure

We proceed as in ref. [22], where a general matrix with two texture zeroes, representing mass matrices of the basic S_3 models,

$$\begin{pmatrix} 0 & a & 0 \\ a^* & b & c \\ 0 & c^* & d \end{pmatrix}, \tag{23}$$

was diagonalised. However, the models of cases II and III have a non-zero entry in the position $(1,1)$. In order to take these models to the form of Eq. (23), we just make a simple shift as follows:

$$\mathcal{M}^f_{Hier} = \mu^f_0 \mathbf{1}_{3\times3} + \widehat{\mathcal{M}}^f_{Hier}. \tag{24}$$

As a starting step in the diagonalisation of the matrices $\mathcal{M}^f_{Hier}$, we write the above shown Hermitian matrix in polar form in terms of a real symmetric matrix $\bar{\mathcal{M}}^f_{Hier}$ and a diagonal matrix of phases

$$\mathcal{P}_f \equiv \mathrm{diag}[1, e^{i\phi_{1f}}, e^{i(\phi_{1f}+\phi_{2f})}], \tag{25}$$

$$\bar{\mathcal{M}}^f_{Hier} \equiv \mathcal{P}^\dagger_f \frac{\widehat{\mathcal{M}}^f_{Hier}}{\sigma_3} \mathcal{P}_f = \mathcal{P}^\dagger_f \begin{pmatrix} 0 & A^f & 0 \\ A^{f*} & B^f & C^f \\ 0 & C^{f*} & D^f \end{pmatrix} \mathcal{P}_f = \begin{pmatrix} 0 & |A^f| & 0 \\ |A^f| & B^f & |C^f| \\ 0 & |C^f| & D^f \end{pmatrix}, \tag{26}$$

where the phase ϕ_{1f} is fixed by $\phi_{1f} = \arctan(|\mu^f_5|/|\mu^f_1|)$, and the phase ϕ_{2f}, remains a real free parameter. Then, as usual, the mass matrix $\bar{\mathcal{M}}^f_{Hier}$ may be brought to a diagonal form by means of an orthogonal transformation,

$$\bar{\mathcal{M}}^f_{Hier} = \mathbf{O}_f \mathrm{diag}[\widetilde{\sigma}^f_1, -\widetilde{\sigma}^f_2, 1]\mathbf{O}^T_f, \tag{27}$$

where $\widetilde{\sigma}^f_i \equiv \sigma^f_i/\sigma^f_3$ are the corresponding real eigenmasses of $\bar{\mathcal{M}}^f_{Hier}$ and $\mathbf{O}_f$ is a real orthogonal matrix. Hence, our unitary matrix, which takes us from the hierarchical basis to the basis where the matrix $\bar{\mathcal{M}}^f_{Hier}$ is diagonal, is

$$\mathbf{U}_f = \mathbf{O}^T_f \mathcal{P}_f. \tag{28}$$

4HDM: $G_{SM} \otimes S_3$

Name	$\mathcal{F}_L$	$\mathcal{F}_R$	Mass matrix (FB)	Possible mass textures
A	$\mathbf{2},\ 1_{\mathbf{S}}$	$\mathbf{2},\ 1_{\mathbf{S}}$	$\begin{pmatrix} \mu_1^f+\mu_2^f & \mu_4^f+\mu_5^f & \mu_6^f \\ \mu_4^f-\mu_5^f & \mu_1^f-\mu_2^f & \mu_7^f \\ \mu_8^f & \mu_9^f & \mu_3^f \end{pmatrix}$	$\begin{pmatrix} 0 & \mu_2^f sc\,(3-t^2) +\mu_5^f & 0 \\ \mu_2^f sc\,(3-t^2) -\mu_5^f & -2\mu_2^f c^2\,(1-3t^2) & \mu_7^f/c \\ 0 & \mu_7^{f*}/c & \mu_3^f-\mu_1^f-\mu_2^f c^2(1-3t^2) \end{pmatrix}$
$A^{'}$				$\begin{pmatrix} 0 & \frac{2}{\sqrt{3}}\mu_2^f+\mu_5^f & 0 \\ \frac{2}{\sqrt{3}}\mu_2^f-\mu_5^f & 0 & \frac{2}{\sqrt{3}}\mu_7^f \\ 0 & \frac{2}{\sqrt{3}}\mu_8^f & \mu_3^f-\mu_1^f \end{pmatrix}$
B	$\mathbf{2},\ 1_{\mathbf{A}}$	$\mathbf{2},\ 1_{\mathbf{A}}$	$\begin{pmatrix} \mu_1^f+\mu_2^f & \mu_4^f+\mu_5^f & \mu_7^f \\ \mu_4^f-\mu_5^f & \mu_1^f-\mu_2^f & -\mu_6^f \\ \mu_9^f & -\mu_8^f & \mu_3^f \end{pmatrix}$	$\begin{pmatrix} 0 & -\mu_4^f c^2\,(1-3t^2) +\mu_5^f & 0 \\ -\mu_4^f c^2\,(1-3t^2) -\mu_5^f & 2\mu_4^f cs\,(3-t^2) & -\mu_6^f/c \\ 0 & -\mu_6^{f*}/c & \mu_3^f-\mu_1^f+\mu_4^f sc(3-t^2) \end{pmatrix}$
$B^{'}$				$\begin{pmatrix} 0 & -2\mu_4^f+\mu_5^f & 0 \\ -2\mu_4^f-\mu_5^f & 0 & -2\mu_6^f \\ 0 & -2\mu_8^f & \mu_3^f-\mu_1^f \end{pmatrix}$
C	$\mathbf{2},\ 1_{\mathbf{A}}$	$\mathbf{2},\ 1_{\mathbf{S}}$	$\begin{pmatrix} \mu_1^f+\mu_2^f & \mu_4^f+\mu_5^f & \mu_6^f \\ \mu_4^f-\mu_5^f & \mu_1^f-\mu_2^f & \mu_7^f \\ \mu_9^f & -\mu_8^f & \nu_3^f \end{pmatrix}$	$\begin{pmatrix} 0 & A_{12} & 0 \\ A_{21} & A_{22} & A_{23} \\ A_{32} & 0 & A_{33}(\mu_3^f \to \nu_3^f) \end{pmatrix}$, $\begin{pmatrix} 0 & B_{12} & B_{23} \\ B_{21} & B_{22} & 0 \\ 0 & B_{32} & B_{33}(\mu_3^f \to \nu_3^f) \end{pmatrix}$
$C^{'}$				$\begin{pmatrix} 0 & A_{12}^{'} & 0 \\ A_{21}^{'} & 0 & A_{23}^{'} \\ A_{32}^{'} & 0 & A_{33}^{'}(\mu_3^f \to \nu_3^f) \end{pmatrix}$, $\begin{pmatrix} 0 & B_{12}^{'} & B_{23}^{'} \\ B_{21}^{'} & 0 & 0 \\ 0 & B_{32}^{'} & B_{33}^{'}(\mu_3^f \to \nu_3^f) \end{pmatrix}$
D	$\mathbf{2},\ 1_{\mathbf{S}}$	$\mathbf{2},\ 1_{\mathbf{A}}$	$\begin{pmatrix} \mu_1^f+\mu_2^f & \mu_4^f+\mu_5^f & \mu_7^f \\ \mu_4^f-\mu_5^f & \mu_1^f-\mu_2^f & -\mu_6^f \\ \mu_8^f & \mu_9^f & \nu_3^f \end{pmatrix}$	$\begin{pmatrix} 0 & A_{12} & A_{23} \\ A_{21} & A_{22} & 0 \\ 0 & A_{32} & A_{33}(\mu_3^f \to \nu_3^f) \end{pmatrix}$, $\begin{pmatrix} 0 & B_{12} & 0 \\ B_{21} & B_{22} & B_{23} \\ B_{32} & 0 & B_{33}(\mu_3^f \to \nu_3^f) \end{pmatrix}$
$D^{'}$				$\begin{pmatrix} 0 & A_{12}^{'} & A_{23}^{'} \\ A_{21}^{'} & 0 & 0 \\ 0 & A_{32}^{'} & A_{33}^{'}(\mu_3^f \to \nu_3^f) \end{pmatrix}$, $\begin{pmatrix} 0 & B_{12}^{'} & 0 \\ B_{21}^{'} & 0 & B_{23}^{'} \\ B_{32}^{'} & 0 & B_{33}^{'}(\mu_3^f \to \nu_3^f) \end{pmatrix}$

Table 4: Mass matrices of S_3-invariant flavour models with four Higgs $SU(2)_L$ doublets which are assigned to all the S_3 irreducible representations, $\mathcal{H}_{AW} \oplus \mathcal{H}_{SW} \oplus \mathcal{H}_{DW}$. We denote $\mu_1^f \equiv \sqrt{2} Y_2^f v_S$, $\mu_2^f \equiv Y_3^f w_2$, $\mu_3^f \equiv 2 Y_1^f v_S$, $\mu_4^f \equiv Y_3^f w_1$, $\mu_5^f \equiv \sqrt{2} Y_4^f v_A$, $\mu_6^f \equiv \sqrt{2} Y_5^f w_1$, $\mu_7^f \equiv \sqrt{2} Y_5^f w_2$, $\mu_8^f \equiv \sqrt{2} Y_6^f w_1$, $\mu_9^f \equiv \sqrt{2} Y_6^f w_2$, and $\nu_3^f \equiv 2 Y_1^f v_A$. In all cases it is assumed that the mass eigenvalues follow a normal order in terms of magnitudes. To simplify the notation, X_{ij} denotes the entry (i,j) in X which is any of the mass textures shown in Table 1. We have denoted $c = \cos\theta$ and $s = \sin\theta$. The only choices of S_3 assignments that may produce a viable model are those where both left- and right-handed parts share the same assignment, as the first and second cases. The primed matrix elements, A_{ij}' or B_{ij}', are particular cases of the unprimed ones, A_{ij} or B_{ij}, with $\theta = \pi/6$ or $\theta = \pi/3$, respectively.

We follow the procedure of ref. [22]. Using the three invariants of the generic real mass matrix $\bar{\mathcal{M}}^f_{Hier}$

$$\begin{aligned} \mathrm{Tr}[\bar{\mathcal{M}}^f_{Hier}] &= \widetilde{\sigma}^f_1 - \widetilde{\sigma}^f_2 + 1 \ , \\ \mathrm{Det}[\bar{\mathcal{M}}^f_{Hier}] &= -\widetilde{\sigma}^f_1 \widetilde{\sigma}^f_2 \ , \\ \mathrm{Tr}[(\bar{\mathcal{M}}^f_{Hier})^2] &= (\widetilde{\sigma}^f_1)^2 + (\widetilde{\sigma}^f_2)^2 + 1 \ , \end{aligned} \tag{29}$$

its parameters, $|A^f|$, B^f, $|C^f|$, and D^f may be expressed in terms of the eigenvalues, $\widetilde{\sigma}^f_i$,

$$\begin{aligned} |A^f| &= \sqrt{\frac{\widetilde{\sigma}^f_1 \widetilde{\sigma}^f_2}{D^f - \tilde{\mu}^f_0}}, \\ B^f - \tilde{\mu}_0 &= 1 + \widetilde{\sigma}^f_1 - \widetilde{\sigma}^f_2 - (D^f - \tilde{\mu}^f_0), \\ |C^f|^2 &= \frac{1 - (D^f - \tilde{\mu}^f_0)}{D^f - \tilde{\mu}^f_0}(D^f - \tilde{\mu}^f_0 - \widetilde{\sigma}^f_1)(D^f - \tilde{\mu}^f_0 - \widetilde{\sigma}^f_2), \end{aligned} \tag{30}$$

where we have defined $\tilde{\mu}^f_0 \equiv \mu^f_0/\sigma^f_3$. To simplify the notation, we define the free parameter δ_f through the following relation

$$\delta_f \equiv 1 - (D^f - \tilde{\mu}_0), \tag{31}$$

which indeed, together with Eq. (30), allows us to write the mass matrix $\widehat{\mathcal{M}}^f_{S_3}$ in terms of its invariants and just one free parameter δ_f

$$\bar{\mathcal{M}}^f_{Hier} = \begin{pmatrix} 0 & \sqrt{\frac{\widetilde{\sigma}^f_1 \widetilde{\sigma}^f_2}{1-\delta_f}} & 0 \\ \sqrt{\frac{\widetilde{\sigma}^f_1 \widetilde{\sigma}^f_2}{1-\delta_f}} & \widetilde{\sigma}^f_1 - \widetilde{\sigma}^f_2 + \delta_f & \sqrt{\frac{\delta_f}{1-\delta_f}\xi^f_1 \xi^f_2} \\ 0 & \sqrt{\frac{\delta_f}{1-\delta_f}\xi^f_1 \xi^f_2} & 1 - \delta_f \end{pmatrix}, \tag{32}$$

in this expression, we have made the following identifications[2]

$$\xi^f_1 \equiv 1 - \widetilde{\sigma}^f_1 - \delta_f, \quad \xi^f_2 \equiv 1 + \widetilde{\sigma}^f_2 - \delta_f \ , \tag{33}$$

such that, δ_f is a measure of the splitting of the two small masses in the first two families in the S_3 doublet as a fraction of the mass of the third family in the S_3 singlet. Therefore, the following hierarchy among the $\delta' s$ for the different kinds of fermions:

$$1 >> \delta_\nu > \delta_l > \delta_d > \delta_u \ , \tag{34}$$

---

[2] In order to make a direct comparison with the notation used in previous publications [16, 22, 66], a change of labels $f \leftrightarrow i$ and $\xi^f_i \leftrightarrow f_i$ must be done, everything else remains the same.

is to be expected. Note that the form of the matrix in Eq. (32) is completely analogous to the mass matrix discussed in Eq. (17) of ref. [22], just with the replacement $\sigma_i \to m_i$. Therefore the diagonalising procedure will follow exactly as in ref. [22], and consequently, the form of the CKM matrix will be the same, we just need to replace m_i by σ_i and take into account the appearance of a new phase ϕ_1. We should bear in mind that σ_i are shifted masses, so in Eq. (32) there are three physical invariants involved and two free parameters, δ_f and $\tilde{\mu}_0^f$. The CKM matrix should contain only one physical phase, the CP violating phase, which means that if there are two parametric phases, ϕ_1 and ϕ_2, the CP violating phase will be a combination of both.

In what follows we describe the general procedure to find the diagonalising matrices for all the cases considered. We then proceed to give the specific details for the cases I through III, mentioned in section 4.

5.3.1 Case I: A single Higgs field

In this case, we have only one Higgs field transforming as $1_{\mathbf{s}}$. There is no Higgs field assigned to the anti-symmetric representation, $1_{\mathbf{A}}$, which translates into the vanishing of ϕ_{1f}. Also, in this case there are no shift parameters μ_0^f for $f = u,\ d$.

5.3.2 Case II: Three Higgs fields

In this case, when the left- and right-handed parts of the fermionic fields of the third family are assigned to the singlet symmetric representation of S_3, there cannot be a Higgs field transforming as $1_{\mathbf{A}}$, therefore the phase ϕ_{1f} vanishes. However, there are shifts μ_0^f, which in principle are non-vanishing.

5.3.3 Case III: Four Higgs fields

In this case we have a fourth Higgs field assigned to the anti-symmetric singlet irrep $1_{\mathbf{A}}$, which produces the μ_5^f parameter in the mass matrices shown in Table 4. In cases A and B in Table 4, we find that after reparametrizing the corresponding mass matrices in terms of the mass eigenvalues, the resulting reparametrized mass matrices are equal. In the reparametrized form, the following inequality holds $\bar{\mathcal{M}}_{Hier}^f[2,2] > \bar{\mathcal{M}}_{Hier}^f[1,2]$ and this inequality implies that either μ_5^f vanishes or the relation $w_1^2 = 3w_2^2$ is satisfied.

In this work we will avoid taking a particular value for the rotation angle, and in consequence we will assume that μ_5^f vanishes. Therefore, the Higgs transforming as the anti-symmetric singlet representation, $1_{\mathbf{A}}$, does not contribute to the Yukawa matrix and the phase ϕ_{1f} does not appear. Hence, the mass matrix, $\bar{\mathcal{M}}_{Hier}^f$, has only one CP violating phase ϕ_{2f} and the parameter δ_f is now constrained to satisfy

$$G_f(\delta_f, \widetilde{\sigma}_i{}^f)t^2(3-t^2)^2 + 4\widetilde{\sigma}_1^f\widetilde{\sigma}_2^f(1-3t^2)^2 = 0, \tag{35}$$

or

$$G_f(\delta_f, \widetilde{\sigma}_i{}^f)(1-3t^2)^2 + 4\widetilde{\sigma}_1^f\widetilde{\sigma}_2^f t^2(3-t^2)^2 = 0, \tag{36}$$

for cases A or B, respectively, where $G_f(\delta_f, \widetilde{\sigma}_i{}^f) = \delta_f^3 - [1-2(\widetilde{\sigma}_1^f - \widetilde{\sigma}_2^f)]\delta_f^2 + (\widetilde{\sigma}_1^f - \widetilde{\sigma}_2^f)(\widetilde{\sigma}_1^f - \widetilde{\sigma}_2^f - 2)\delta_f - (\widetilde{\sigma}_1^f - \widetilde{\sigma}_2^f)^2$.

6 Form of the CKM matrix

The V_{CKM} matrix is defined as

$$V_{CKM}^{th} = \mathbf{U}_{u_L}^\dagger \mathbf{U}_{d_L} = \mathbf{O}_u^T P^{(u-d)} \mathbf{O}_d, \tag{37}$$

where $P^{(u-d)} = \mathrm{diag}[1, e^{i\phi_1}, e^{i(\phi_1+\phi_2)}]$ with $\phi_i \equiv \phi_{iu} - \phi_{id}$, and $\mathbf{O}_{u,d}$ are the real orthogonal matrices, Eq. (28), that diagonalise the real symmetric mass matrix of Eq. (32). The substitution of the expressions $\mathbf{O}_f$ [3] in the unitary matrices of Eq. (37) allows us to express the entries in the quark mixing matrix V_{CKM}^{th} as explicit functions of the quark masses

---

[3] This is completely analogous to the expression of Eq. (25) in ref. [22], with the replacements $\widetilde{m}_i \to \widetilde{\sigma}_i$ and $f_i \to \xi_i$.

$$\begin{aligned}
V_{ud}^{th} &= \sqrt{\frac{\widetilde{\sigma}_c\widetilde{\sigma}_s\xi_1^u\xi_1^d}{\mathcal{D}_{1u}\mathcal{D}_{1d}}} + \sqrt{\frac{\widetilde{\sigma}_u\widetilde{\sigma}_d}{\mathcal{D}_{1u}\mathcal{D}_{1d}}}\left(\sqrt{(1-\delta_u)\,(1-\delta_d)\,\xi_1^u\xi_1^d} + \sqrt{\delta_u\delta_d\xi_2^u\xi_2^d}e^{i\phi_2}\right)e^{i\phi_1}, \\
V_{us}^{th} &= -\sqrt{\frac{\widetilde{\sigma}_c\widetilde{\sigma}_d\xi_1^u\xi_2^d}{\mathcal{D}_{1u}\mathcal{D}_{2d}}} + \sqrt{\frac{\widetilde{\sigma}_u\widetilde{\sigma}_s}{\mathcal{D}_{1u}\mathcal{D}_{2d}}}\left(\sqrt{(1-\delta_u)\,(1-\delta_d)\,\xi_1^u\xi_2^d} + \sqrt{\delta_u\delta_d\xi_2^u\xi_1^d}e^{i\phi_2}\right)e^{i\phi_1}, \\
V_{ub}^{th} &= \sqrt{\frac{\widetilde{\sigma}_c\widetilde{\sigma}_d\widetilde{\sigma}_s\delta_d\xi_1^u}{\mathcal{D}_{1u}\mathcal{D}_{3d}}} + \sqrt{\frac{\widetilde{\sigma}_u}{\mathcal{D}_{1u}\mathcal{D}_{3d}}}\left(\sqrt{(1-\delta_u)\,(1-\delta_d)\,\delta_d\xi_1^u} - \sqrt{\delta_u\xi_2^u\xi_1^d\xi_2^d}e^{i\phi_2}\right)e^{i\phi_1}, \\
V_{cd}^{th} &= -\sqrt{\frac{\widetilde{\sigma}_u\widetilde{\sigma}_s\xi_2^u\xi_1^d}{\mathcal{D}_{2u}\mathcal{D}_{1d}}} + \sqrt{\frac{\widetilde{\sigma}_c\widetilde{\sigma}_d}{\mathcal{D}_{2u}\mathcal{D}_{1d}}}\left(\sqrt{(1-\delta_u)\,(1-\delta_d)\,\xi_2^u\xi_1^d} + \sqrt{\delta_u\delta_d\xi_1^u\xi_2^d}e^{i\phi_2}\right)e^{i\phi_1}, \\
V_{cs}^{th} &= \sqrt{\frac{\widetilde{\sigma}_u\widetilde{\sigma}_d\xi_2^u\xi_2^d}{\mathcal{D}_{2u}\mathcal{D}_{2d}}} + \sqrt{\frac{\widetilde{\sigma}_c\widetilde{\sigma}_s}{\mathcal{D}_{2u}\mathcal{D}_{2d}}}\left(\sqrt{(1-\delta_u)\,(1-\delta_d)\,\xi_2^u\xi_2^d} + \sqrt{\delta_u\delta_d\xi_1^u\xi_1^d}e^{i\phi_2}\right)e^{i\phi_1}, \\
V_{cb}^{th} &= -\sqrt{\frac{\widetilde{\sigma}_u\widetilde{\sigma}_d\widetilde{\sigma}_s\delta_d\xi_2^u}{\mathcal{D}_{2u}\mathcal{D}_{3d}}} + \sqrt{\frac{\widetilde{\sigma}_c}{\mathcal{D}_{2u}\mathcal{D}_{3d}}}\left(\sqrt{(1-\delta_u)\,(1-\delta_d)\,\delta_d\xi_2^u} - \sqrt{\delta_u\xi_1^u\xi_1^d\xi_2^d}e^{i\phi_2}\right)e^{i\phi_1}, \\
V_{td}^{th} &= \sqrt{\frac{\widetilde{\sigma}_u\widetilde{\sigma}_c\widetilde{\sigma}_s\delta_u\xi_1^d}{\mathcal{D}_{3u}\mathcal{D}_{1d}}} + \sqrt{\frac{\widetilde{\sigma}_d}{\mathcal{D}_{3u}\mathcal{D}_{1d}}}\left(\sqrt{\delta_u\,(1-\delta_u)\,(1-\delta_d)\,\xi_1^d} - \sqrt{\delta_d\xi_1^u\xi_2^u\xi_2^d}e^{i\phi_2}\right)e^{i\phi_1}, \\
V_{ts}^{th} &= -\sqrt{\frac{\widetilde{\sigma}_u\widetilde{\sigma}_c\widetilde{\sigma}_d\delta_u\xi_2^d}{\mathcal{D}_{3u}\mathcal{D}_{2d}}} + \sqrt{\frac{\widetilde{\sigma}_s}{\mathcal{D}_{3u}\mathcal{D}_{2d}}}\left(\sqrt{\delta_u\,(1-\delta_u)\,(1-\delta_d)\,\xi_2^d} - \sqrt{\delta_d\xi_1^u\xi_2^u\xi_1^d}e^{i\phi_2}\right)e^{i\phi_1}, \\
V_{tb}^{th} &= \sqrt{\frac{\widetilde{\sigma}_u\widetilde{\sigma}_c\widetilde{\sigma}_d\widetilde{\sigma}_s\delta_u\delta_d}{\mathcal{D}_{3u}\mathcal{D}_{3d}}} + \left(\sqrt{\frac{\xi_1^u\xi_2^u\xi_1^d\xi_2^d}{\mathcal{D}_{3u}\mathcal{D}_{3d}}} + \sqrt{\frac{\delta_u\delta_d(1-\delta_u)(1-\delta_d)}{\mathcal{D}_{3u}D_{3d}}}e^{i\phi_2}\right)e^{i\phi_1}\ ,
\end{aligned} \tag{38}$$

with

$$\begin{aligned}
\xi_1^{u,d} &= 1-\widetilde{\sigma}_{u,d}-\delta_{u,d}, \quad \xi_2^{u,d} = 1+\widetilde{\sigma}_{c,s}-\delta_{u,d}, \\
\mathcal{D}_{1(u,d)} &= (1-\delta_{u,d})(\widetilde{\sigma}_{u,d}+\widetilde{\sigma}_{c,s})(1-\widetilde{\sigma}_{u,d}), \\
\mathcal{D}_{2(u,d)} &= (1-\delta_{u,d})(\widetilde{\sigma}_{u,d}+\widetilde{\sigma}_{c,s})(1+\widetilde{\sigma}_{c,s}), \\
\mathcal{D}_{3(u,d)} &= (1-\delta_{u,d})(1-\widetilde{\sigma}_{u,d})(1+\widetilde{\sigma}_{c,s}).
\end{aligned} \tag{39}$$

6.1 Case I: A single Higgs field

For this case, the form of the CKM matrix corresponds to that of Eq. (38) with $\phi_2 = 0$, μ_0^f vanishing and $m_i^f = \sigma_i^f$.

6.2 Case II: Three Higgs fields

For the cases A and B in Tab. 1, we can parameterize the CKM matrix with a non-vanishing phase $\phi_2 = 0$, and since for these cases μ_0^f is not zero, we set $m_i^f = \mu_0^f + \sigma_i^f$.

6.3 Case III: Four Higgs fields

In this case, we can parameterize the CKM matrix as in cases A and B, again with a non-vanishing phase $\phi_2 = 0$, following the discussion in Sec. (5.3.3). In these cases μ_0^f does not vanish and we set $m_i^f = \mu_0^f + \sigma_i^f$.

7 The S_3 models compared with experimental data

7.1 Experimental status

Over the last decade, there has been a remarkable improvement in the precision and quality of the measurements of the elements of the Cabibbo-Kobayashi-Maskawa (CKM) mixing matrix, the quark masses, and their uncertainties. At present, any model for quark masses must provide a detailed analysis of their predictions or have the ability to reproduce or to accommodate the ever increasing precision of the experimental results. In the following subsections, we present a brief overview of the experimental status of quark masses and their mixing. We explain how we confront this information with the exact analytical expressions we found, given in terms of quark mass ratios, of the CKM mixing matrix elements. Then, we comment on the results of the χ^2 fits for the S_3 models presented in this work.

In order to do this analysis, we will use the running quark masses at the electroweak scale which we fix at the M_Z scale. We obtained the numerical values of the running quark masses at M_Z using the RunDec program [70] and the most recent PDG values [52], which are presented at different scales. For comparison, we also quote the results on values of the quark masses 2010-2011, reported in ref. [55] and in the 2011 online version of the PDG. We present the results in Tab. 5. We note that while most part of the central values of $m_i(M_Z)$ are compatible with those cited in ref. [71], the uncertainties have been greatly reduced in the last analysis.

7.2 Fitting procedure

We construct the χ^2 function as

$$\chi^2 = \frac{\left(|V_{ud}^{\rm th}| - |V_{ud}|\right)^2}{\sigma_{V_{ud}}^2} + \frac{\left(|V_{us}^{\rm th}| - |V_{us}|\right)^2}{\sigma_{V_{us}}^2} + \frac{\left(|V_{ub}^{\rm th}| - |V_{ub}|\right)^2}{\sigma_{V_{ub}}^2} + \frac{\left(\mathcal{J}_q^{\rm th} - \mathcal{J}_q\right)^2}{\sigma_{\mathcal{J}_q}^2}, \tag{40}$$

where the quantities with super-index "th" are the complete expressions for the CKM elements, as given by the S_3 models, and those without, the experimental quantities along with their

	2011 values [GeV]	2012 values [GeV]	$m_f^{\overline{MS}}(M_Z)$ 2011 [GeV]	$m_f^{\overline{MS}}(M_Z)$ 2012 [GeV]
m_t	$172.0 \pm 0.6 \pm 0.9$	$172.85 \pm 0.71 \pm 0.85$	171.13 ± 1.19	171.07 ± 1.21
m_b^{OS}	$4.67^{+0.18}_{-0.06}$	4.65 ± 0.03		
m_b	$4.19^{+0.18}_{-0.06}$	4.18 ± 0.03	2.84 ± 0.04	2.85 ± 0.04
m_c	$1.29^{+0.05}_{-0.11}$	1.275 ± 0.0025	0.616 ± 0.064	0.626 ± 0.0094
m_s	$0.100^{+0.030}_{-0.020}$	0.095 ± 0.005	0.061 ± 0.015	0.055 ± 0.0033
m_d	$(0.0041, 0.0057)$	$4.8^{+0.7}_{-0.3} \times 10^{-3}$	0.00284 ± 0.00050	0.0028 ± 0.0005
m_u	$(0.0017, 0.0031)$	$2.3^{+0.7}_{-0.5} \times 10^{-3}$	0.00139 ± 0.00042	0.0014 ± 0.0005

Table 5: Values of quark masses, in GeV, as appear in the online 2011 version of the PDG and in [55], and the updated values of 2012 [52]. The values quoted at M_Z, were obtained with the program RunDec [70] at four loops in the running of α_s. For the 2011 data, note that with the use of the chiral perturbation relation involving the parameter $Q = 23 \pm 2$, we obtain $m_u(M_Z) = 0.00130 \pm 0.00047$, which is now compatible with the value obtained directly from the PDG and the evolution up to M_Z.

uncertainty $\sigma_{V_{ij}}$. We consider the following experimental CKM values

$$\begin{array}{llll}
2011: & |V_{ud}| = 0.97428 \pm 0.00015, & 2012: & |V_{ud}| = 0.97427 \pm 0.00015, \\
 & |V_{us}| = 0.2253 \pm 0.007, & & |V_{us}| = 0.2253 \pm 0.007, \\
 & |V_{ub}| = 0.00347 \pm 0.00014, & & |V_{ub}| = 0.00351 \pm 0.00015, \\
 & J = (2.91 \pm 0.155) \times 10^{-5}, & & J = (2.96 \pm 0.18) \times 10^{-5}\ ,
\end{array} \tag{41}$$

which correspond to a unitary CKM matrix in the case of three generations of quarks. Since unitary of the CKM mixing matrix is assumed, there is no need to make the fit to the entire matrix but only to four observables. The theoretical expressions of the CKM elements are given in terms of the mass ratios, $\widetilde{m_i}$, Eq. (33), or the parameters $\widetilde{\sigma}_i$, Eq. (19), hence the minimisation of the defined χ^2 is a function of the *parameters* $\widetilde{m_i}$, δ_u, δ_d and $\cos\phi_1$. This means that, as a result of the minimisation, there is a *best fit value* for each of those quantities, for which χ^2 takes the minimum value. The mass ratios $\widetilde{m}_i$ are not free parameters. The limits we set correspond to their allowed 3σ regions. We also test if there is convergence when using the (2σ) regions. In the fitting procedure, we used MINUIT from ROOT [72] for the numerical minimisation. The values used for the parameters $\widetilde{m}_i$ are given in Table 6.

	2011	2012
$\widetilde{m_u}\,(M_Z)$	0.0000082 ± 0.0000027	0.0000083 ± 0.0000030
$\widetilde{m_c}\,(M_Z)$	0.0036 ± 0.0004	0.0037 ± 0.00008
$\widetilde{m_d}\,(M_Z)$	0.00098 ± 0.00018	0.00098 ± 0.00017
$\widetilde{m_s}\,(M_Z)$	0.0205 ± 0.0056	0.0190 ± 0.0014

Table 6: Comparison of the values of the mass ratios, at M_Z, in 2011 and 2012.

	$m_f^{\overline{MS}}(M_Z)$		
m_s	0.059 ± 0.0066	$\widetilde{m_s}\,(M_Z)$	0.0205 ± 0.0026
m_d	0.0028 ± 0.0005	$\widetilde{m_d}\,(M_Z)$	0.00098 ± 0.00017
m_u	0.0013 ± 0.0005	$\widetilde{m_u}\,(M_Z)$	0.0000078 ± 0.0000030

Table 7: Changes in the masses of the lightest quarks when using the average of the theoretical determinations of m_s, that is, not including attice determinations. We obtain $m_s(2\text{GeV}) = 0.101 \pm 0.011$ GeV.

7.3 Results

We have proceeded with the minimisation of the χ^2 as follows. We used MINUIT and varied all the parameters $\widetilde{m}_i$, within the 2σ and 3σ ranges given in Tab. 6 and Tab. 7, and δ_u, δ_d as true free parameters.

7.3.1 Case I: A single Higgs field

This case corresponds to the well known case of broken $S_{3L} \otimes S_{3R}$, in the presence of one singlet S_3 Higgs field, which gives rise to an effective mass matrix of the form of Eq. (8). Hence, the CKM matrix we fit is that of Eq. (38) with $\phi_2 = 0$ and $\tilde{\sigma}_i = \tilde{m}_i$.

In one set of fits, we fixed ϕ_1 to $\pi/2$ following previous fits to the quark mass ratios where this value was shown to be the preferred one [16, 17]. However, when allowing the phase ϕ_1 to vary in the region $\cos\phi_1 \in (0, 1)$, the quality of the fits is better for a larger value of $\cos\phi_1$, than for a small value of ϕ_1. Therefore, we present three sets of fits, one when ϕ_1 is fixed to $\pi/2$, another when we allow $\cos\phi_1$ to vary in the region $(-0.5, 0.5)$ and a third one, where we allow $\cos\phi_1$ to vary in the region $(0.5, 1.0)$.

We recall that minimisations with MINUIT rely on setting a starting value for the parameters to fit with a seed close enough to the minimum, therefore if the range of variation of a particular parameter is large, it is difficult to find its best fit point. Additionally, to check the consistency of a minimum, one should remove the limits of the parameters to fit. Unfortunately, if we perform the fit leaving the parameters $\widetilde{m_i}$ completely free to vary without limits, the quality of the fits does not really improve, and most importantly, for these cases it turns out that the best fit point of $\widetilde{m_u}$ is of order 10^{-3}. We mention that the reported values in 2011, by the PDG, of m_u and m_d quoted an uncertainty of about 30% of the central value, so they were difficult to fit. The situation in 2012, particularly for m_s, changed since the uncertainty in the lattice determinations of m_s was reduced down to 5%. In contrast, the theoretical determinations of m_s have an uncertainty of almost 10%. Consequently, in order to assess the impact of lattice and theoretical determinations, we also make fits using only an average of the theoretical determinations.

Case when $\phi_1 = \pi/2$ fixed. We find that for the reported 2012 experimental values of quark masses and mixing, when allowing the mass ratios to vary within their 3σ ranges, for $\widetilde{m}_u$, $\widetilde{m}_c$, and $\widetilde{m}_s$, the χ^2 function attains a minimum within the corresponding 3σ region of each of the parameters above. On the other hand, the BFP of $\widetilde{m}_d$ lies within its 1σ region. The results of this fit are shown in Figs. 1 -2 and the values of the BFPs are given in Tab. 8.

For comparison, we have also performed the fit with the experimental results reported in 2011 by the PDG and with the 2012 results taking into account the theoretical determinations of $\widetilde{m}_s$, Tab. 7. As we can see from the plots in Figs. 1-2 for the former set of data, the χ^2 functions does not really attain a minimum as a function of $\tilde{m}_u$ and $\tilde{m}_c$, when they vary within their 3σ region. On the other hand, the best fit point of $\tilde{m}_d$ lies within its three sigma region, while the best fit point of $\tilde{m}_s$ within its two sigma region. When we take into account the data from 2012 only with the average of the theoretical determination of $\tilde{m}_s$, we notice that the best fit points of $\tilde{m}_u$ lie within their corresponding 3σ region, while the best fit points of $\tilde{m}_d$ and $\tilde{m}_s$ lie within their corresponding 2σ region. The results of this fit are shown in Figs.3-4, the values of the best fit point are given in Tab. 8.

Varying $\cos\phi_1$ in $(-0.5, 0.5)$. When allowing the mass ratios to vary within their 3σ ranges, we find that the χ^2 function does not really reach a minimum as a function of $\widetilde{m}_u$ and $\widetilde{m}_c$, while as a function of $\widetilde{m}_d$ and $\widetilde{m}_s$, it does reach a minimum within their corresponding 1σ region. The results of this fit are shown in Figs. 3-4, the values of the best fit point are given in Tab. 8. For the fit, when taking into account the average of the theoretical determination of $\widetilde{m}_s$, we find that χ^2 attain a minimum only as a function of $\widetilde{m}_d$, whose best fit point lies within its 1σ region. The fit, when using the 2011 data, shows that the χ^2 function attains a minimum as a function of $\widetilde{m}_u$, $\widetilde{m}_d$ and $\widetilde{m}_s$. For $\widetilde{m}_u$, its BFP lies within its 3σ region while for $\widetilde{m}_d$ and $\widetilde{m}_s$, their best fit points lie within their corresponding 2σ region.

Varying $\cos\phi_1$ in $(0.5, 1.0)$. For this fit, when allowing the mass ratios to vary within their 3σ ranges, we find that the χ^2 function attains a minimum as a function of all the mass ratios. For $\widetilde{m}_u$, $\widetilde{m}_c$ and $\widetilde{m}_d$, the minimum lies within their 3σ range. For $\widetilde{m}_d$ the minimum lies within its 1σ range. The results of these fits are shown in Figs. 5-6, the values of the best fit points are given in Tab. 8. When considering the average of the theoretical determination of $\widetilde{m}_s$, we find that χ^2 attains a minimum only as a function of $\widetilde{m}_s$, whose BFP lies within its 1σ region. For the data of 2011, χ^2 attains a minimus for $\widetilde{m}_u$ and $\widetilde{m}_c$ within their corresponding 3σ region, while $\widetilde{m}_d$ within its 1σ region and $\widetilde{m}_s$ within its corresponding 2σ region.

General comments on the quality of the fits. From Figs. 1-4 we can see that the ratio $\widetilde{m}_c$ is not greatly affected by the change in the value of ϕ_1. However, the minimum of χ^2 as a function function of $\widetilde{m}_c$ when $\cos\phi_1 \approx 0.5$, seems to be better behaved as that of a fixed value of ϕ_1 equal to $\pi/2$. When we allow $\widetilde{m}_s$ to vary in the range determined by the uncertainty in

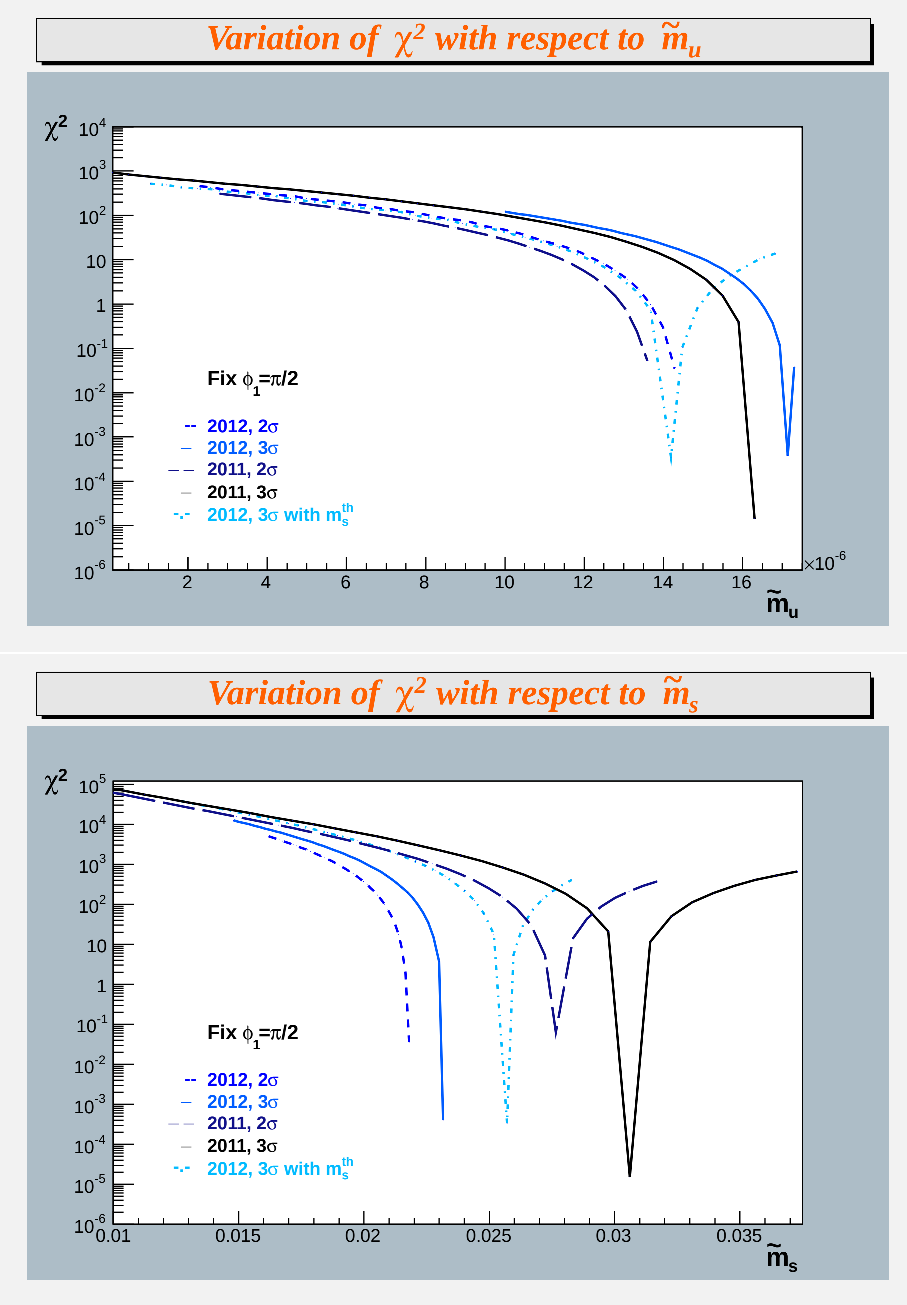

Figure 1: Results of the χ^2 fit as a function of $\widetilde{m}_u$ and $\widetilde{m}_s$ for the case where the phase ϕ_1 is fixed to $\pi/2$. The reported masses of quarks in 2011 give to the ratios $\widetilde{m_u}$ and $\widetilde{m_s}$ an uncertainty of about 30% of their central value, therefore they were difficult to fit. The situation in 2012 has improved, in particular for the strange quark mass $\widetilde{m}_s$ the lattice determinations reduced its uncertainty to 5% of its central value. Since this is quite remarkable, we have also fitted the mass ratios using as limits the values obtained by considering just the theoretical determination of $\widetilde{m}_s$, for which we obtain $m_s(2\text{ GeV}) = 0.101 \pm 0.011$ GeV.

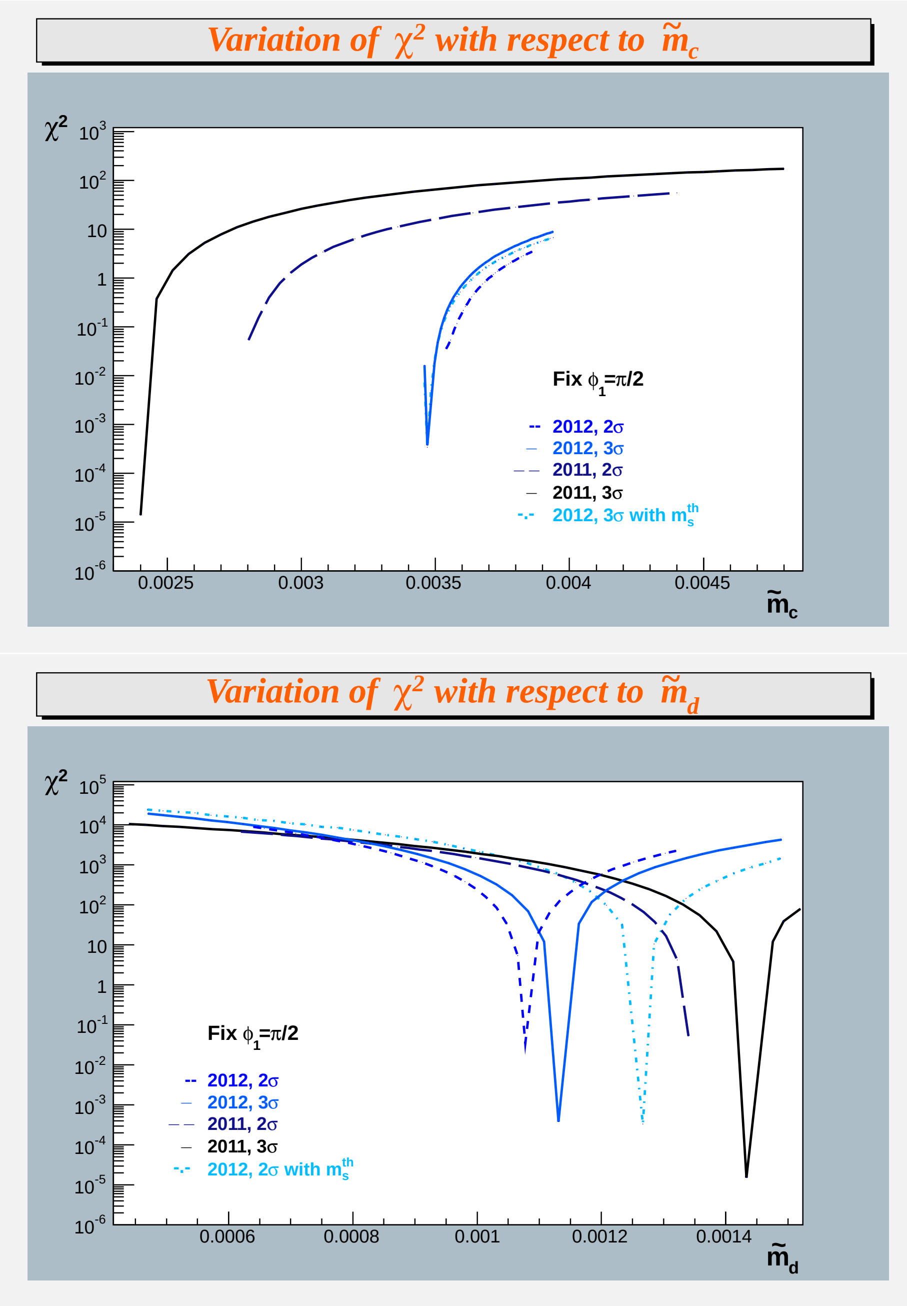

Figure 2: The same as in Fig. 1 for χ^2 fit as a function of $\widetilde{m}_c$ and $\widetilde{m}_d$.

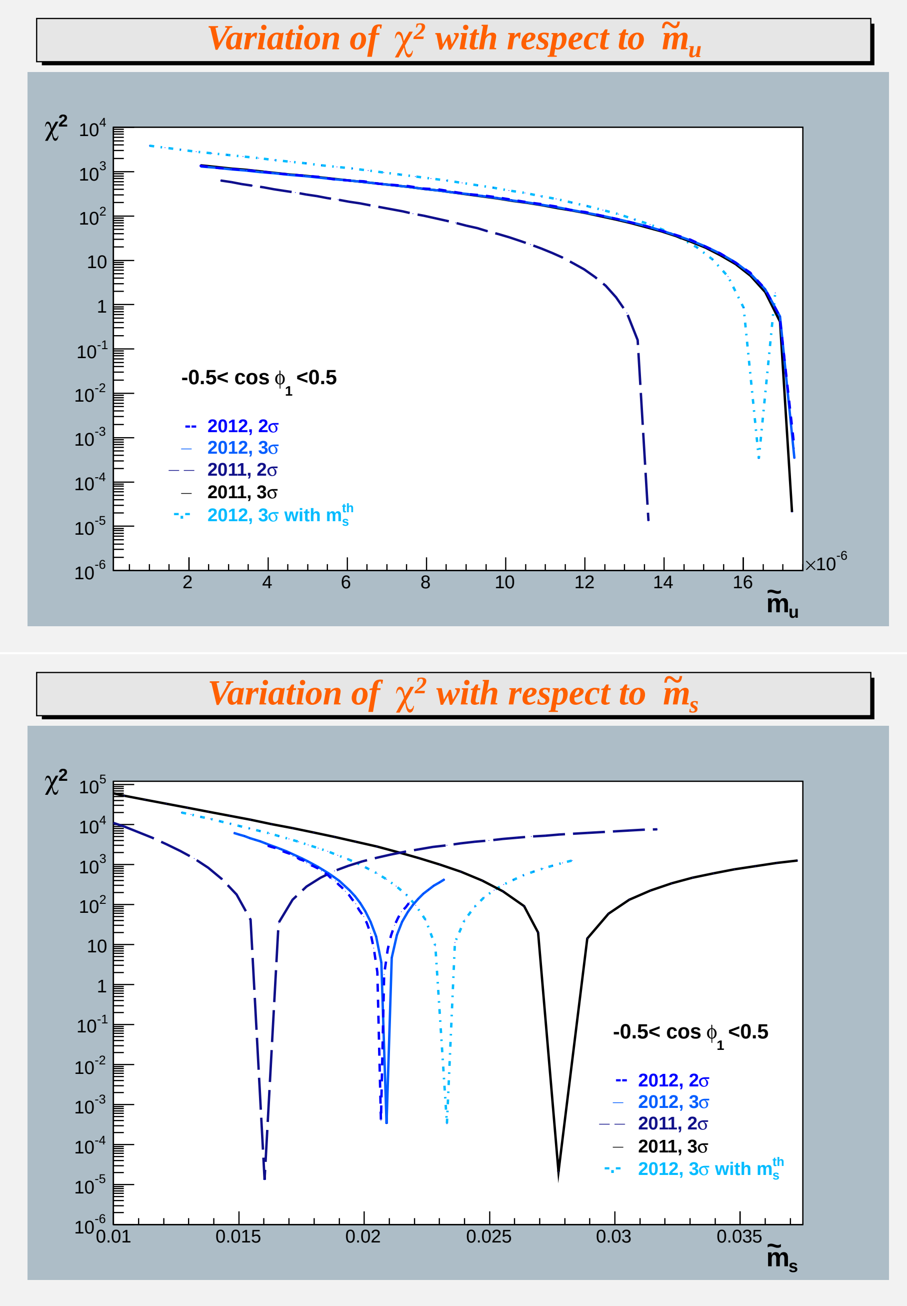

Figure 3: The same as in Fig. 1, except that now $\cos\phi_1$ is allowed to vary in $(-0.5, 0.5)$.

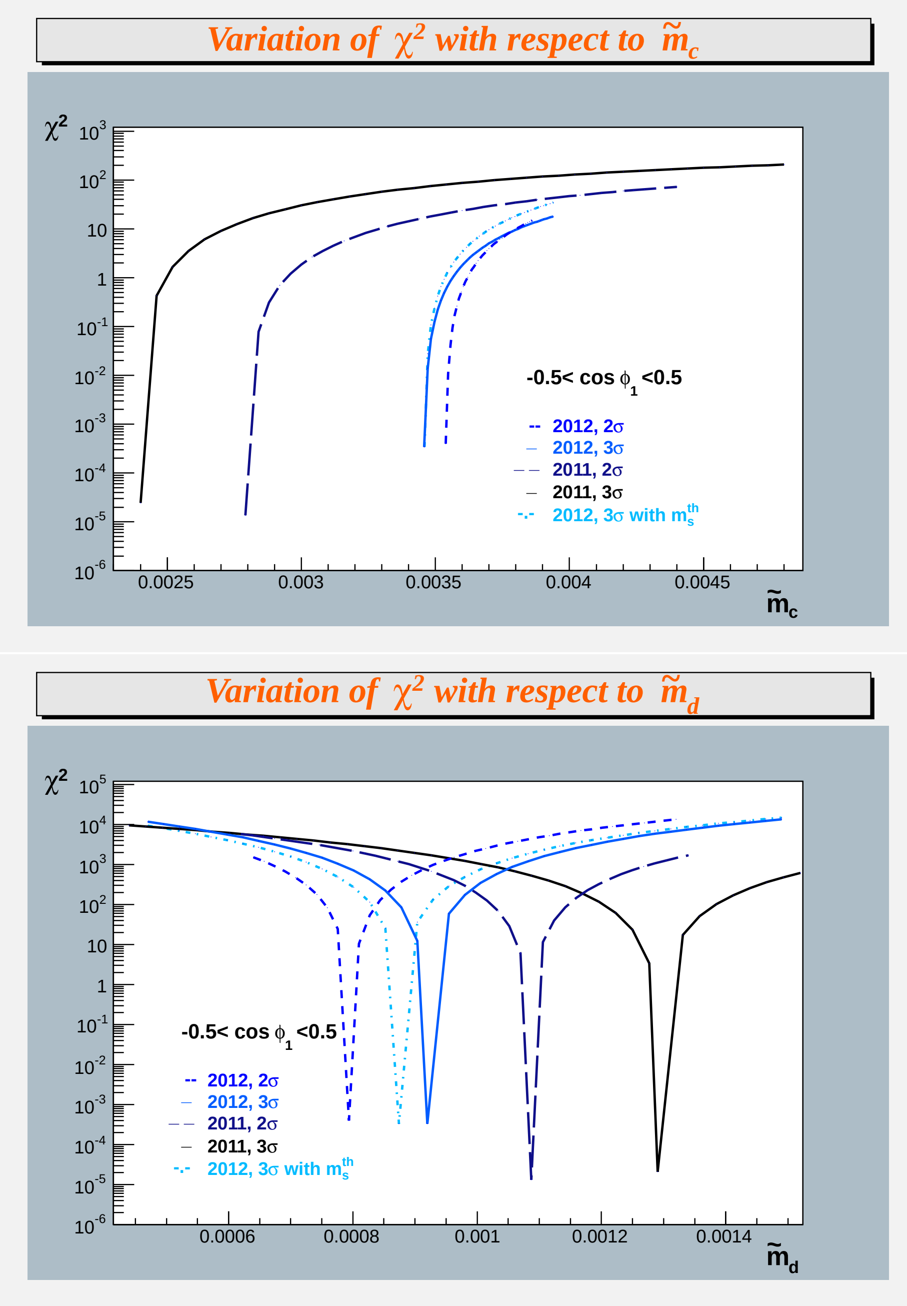

Figure 4: The same as in Fig. 2, except that now $\cos\phi_1$ is allowed to vary in $(-0.5, 0.5)$.

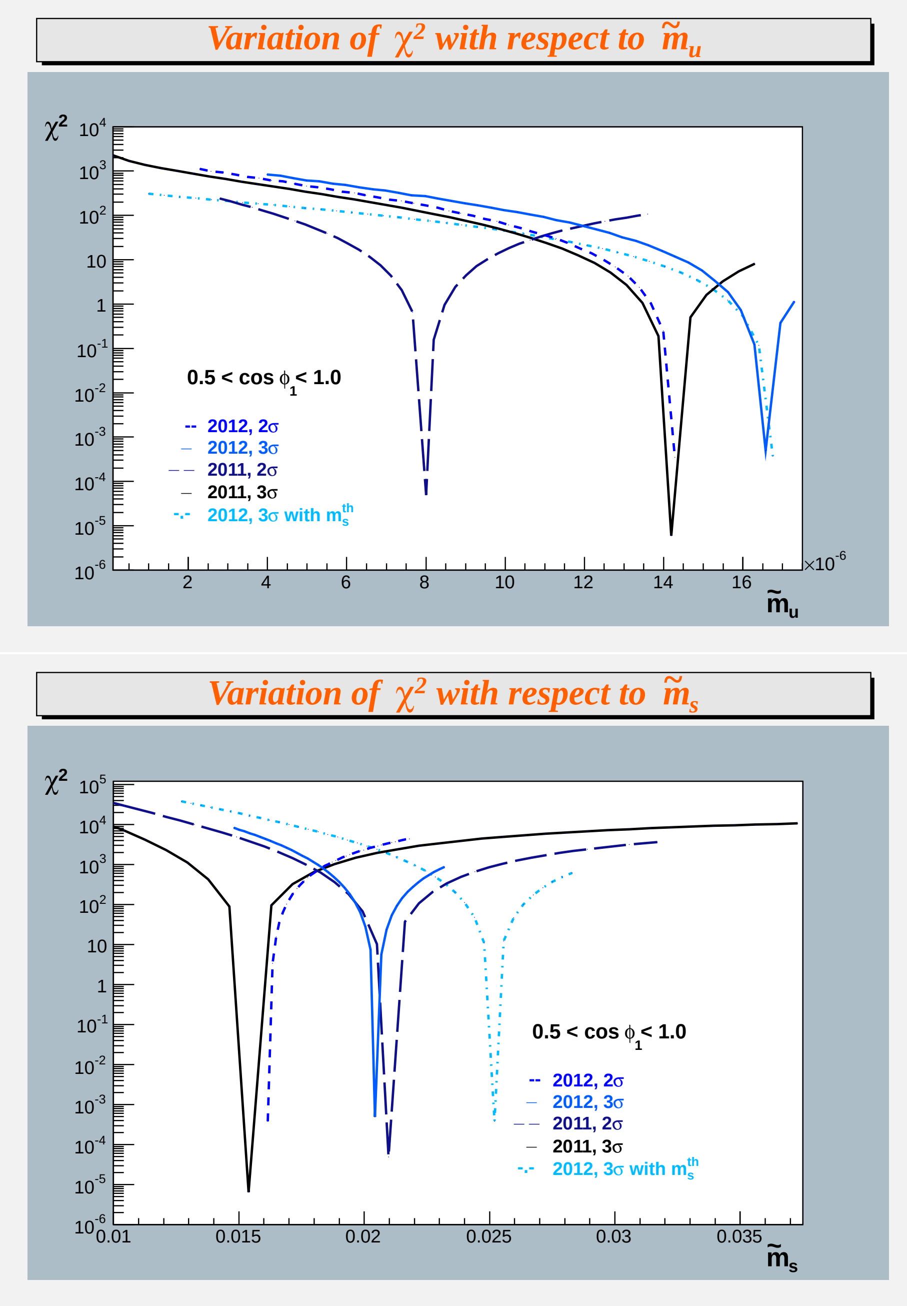

Figure 5: The same as in Figs. 1-4, except that now $\cos\phi_1$ is allowed to vary in the region $(0.5, 1.0)$.

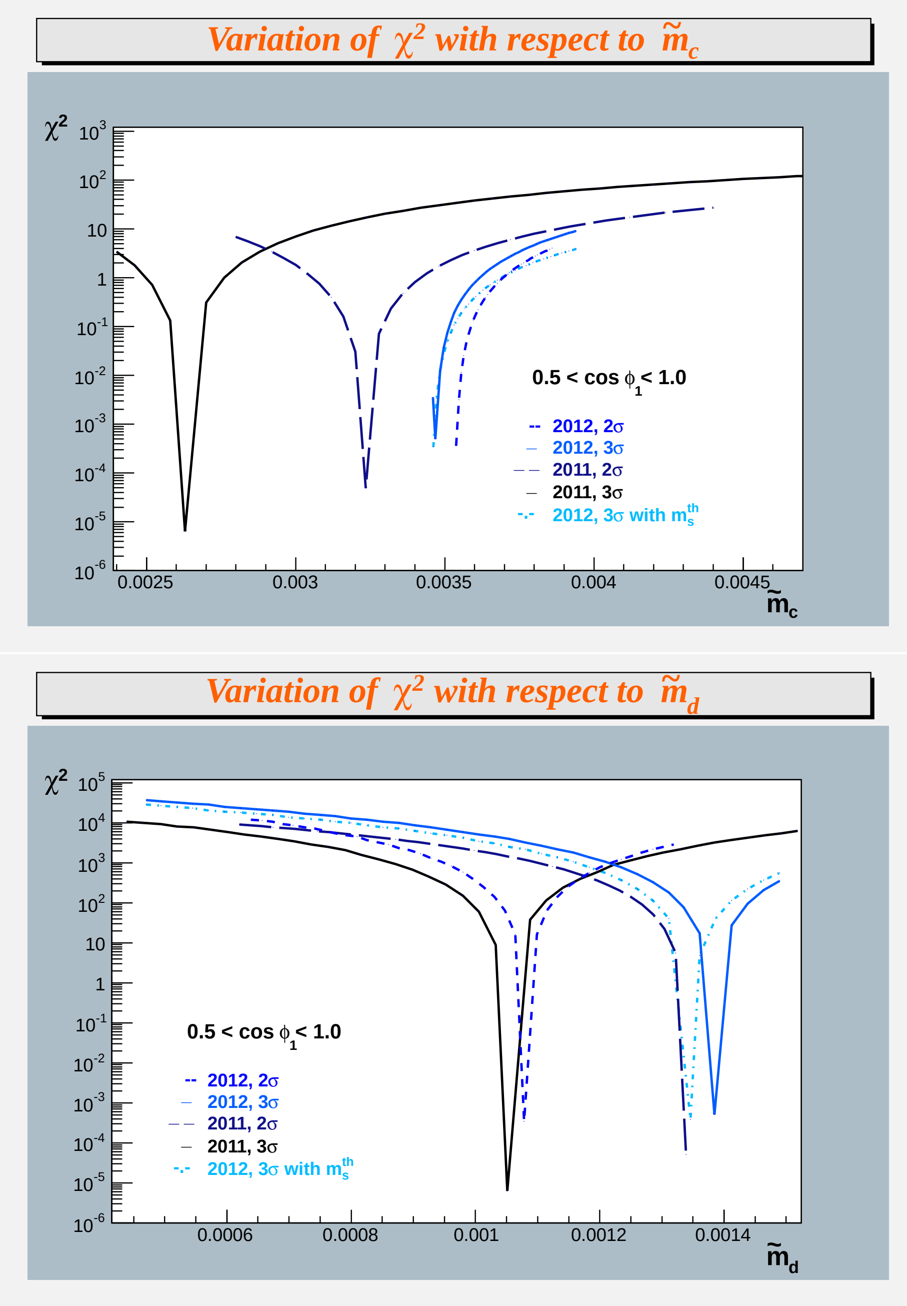

Figure 6: The same as in Figs. 1-4, except that now $\cos\phi_1$ is allowed to vary in the region $(0.5, 1.0)$.

the theoretical determination of m_s, we can see that the preferred region for the fit of $\widetilde{m}_c$ is quite similar to that of 2011. We can also see that the overall quality of the fit is better for the case of $\cos\phi_1$ if it is allowed to vary within $(0.5, 1)$. In fact, if we allow $\cos\phi_1$ to vary within $(0, 1)$, the overall best fit is practically the same as that of the one when $\cos\phi_1$ is allowed to vary within $(0.5, 1)$.

Parameter	Central value	χ^2	Values with restricted precision	χ^2
$\widetilde{m_u}\,(M_Z)$	1.72991×10^{-5}		$(1.73 \pm 0.75) \times 10^{-5}$	
$\widetilde{m_c}\,(M_Z)$	3.46×10^{-3}		$(3.46 \pm 0.43) \times 10^{-3}$	
$\widetilde{m_d}\,(M_Z)$	1.12461×10^{-3}		$(1.12 \pm 0.007) \times 10^{-3}$	
$\widetilde{m_s}\,(M_Z)$	2.32×10^{-2}		$(2.32 \pm 0.84) \times 10^{-2}$	
δ_u	6.05040×10^{-2}		$(6.05 \pm 3.02) \times 10^{-2}$	
δ_d	4.09162×10^{-2}		$(4.09 \pm 2.59) \times 10^{-2}$	
$\cos\phi_1$	0 [Fixed]			
		3.4×10^{-4}		7.4×10^{-1}
$\widetilde{m_u}\,(M_Z)$	1.72960×10^{-5}		$(1.73 \pm 0.06) \times 10^{-6}$	
$\widetilde{m_c}\,(M_Z)$	3.46008×10^{-3}		$(3.46 \pm 0.31) \times 10^{-3}$	
$\widetilde{m_d}\,(M_Z)$	9.19505×10^{-4}		$(9.20 \pm 0.72) \times 10^{-4}$	
$\widetilde{m_s}\,(M_Z)$	2.08735×10^{-2}		$(2.09 \pm 0.01) \times 10^{-2}$	
δ_u	3.48158×10^{-2}		$(3.48 \pm 0.83) \times 10^{-2}$	
δ_d	1.99291×10^{-2}		$(1.99 \pm 0.63) \times 10^{-2}$	
$\cos\phi_1$	-1.42545×10^{-2}		$(-1.42 \pm 1.7) \times 10^{-2}$	
		1.32×10^{-5}		2.4×10^{-2}
$\widetilde{m_u}\,(M_Z)$	1.71856×10^{-5}		$(1.72 \pm 0.78) \times 10^{-6}$	
$\widetilde{m_c}\,(M_Z)$	3.46176×10^{-3}		$(3.46 \pm 0.26) \times 10^{-3}$	
$\widetilde{m_d}\,(M_Z)$	1.05595×10^{-3}		$(1.06 \pm 0.40) \times 10^{-3}$	
$\widetilde{m_s}\,(M_Z)$	1.55660×10^{-2}		$(1.56 \pm 0.72) \times 10^{-2}$	
δ_u	2.50428×10^{-2}		$(2.50 \pm 6.18) \times 10^{-2}$	
δ_d	4.09101×10^{-2}		$(4.09 \pm 7.04 \times 10^{-2}$	
$\cos\phi_1$	5.0×10^{-1}		$(5.0 \pm 3.74) \times 10^{-1}$	
		3.4×10^{-4}		1.6×10^{-1}

Table 8: Results of the fits for Case I, that is the case of a broken $S_{3L} \otimes S_{3R}$ symmetry. Note that when we restrict the precision of the fitted values, we observe a significant change in the value of χ^2.

Interpretation of the parameters $\boldsymbol{\delta_u}$ and $\boldsymbol{\delta_d}$. In this case, the symmetry breaking parameter Z_f, $f = u, d$, which measures the mixture of the singlet and the doublet representations of

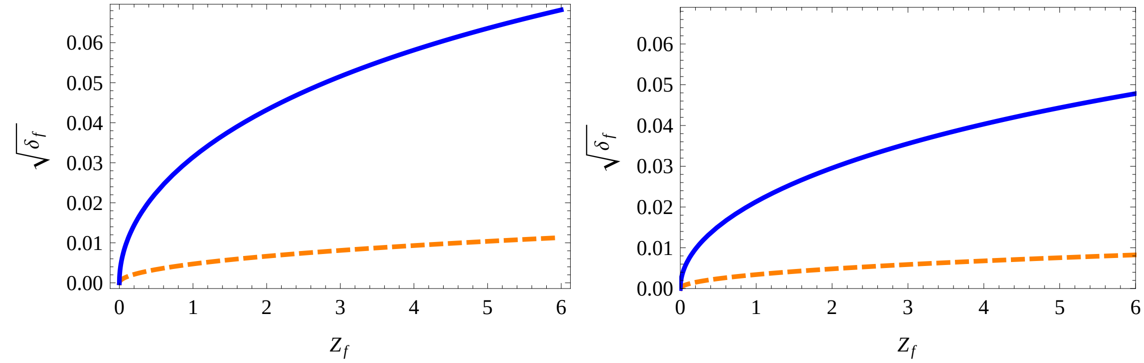

Figure 7: $\sqrt{\delta_f}$, $f = u$ blue (solid) curve, $f = d$ orange (dashed) curve, as a function of Z_f, for one of the three solutions of Eq. (43). The plot on the left corresponds to the plot of 1999 from ref. [16], while the plot on the right corresponds to taking the results, except the value of the parameters δ_f, of the fit of case I for $\phi_1 = \pi/2$, Tab. 8. In this case, we have given as input the value of Z_f and chosen the analogous solution to the 1999 fit for δ_f, using Eq. (43). We see that both solutions are compatible, if we wanted to choose the value of the parameters δ_f as a function of Z_f.

S_3, was defined in ref. [16, 17] as

$$Z_f = \sqrt{\frac{(M_f)_{23}}{(M_f)_{22}}}, \tag{42}$$

and it can be related to δ_f through a cubic equation

$$\begin{aligned} F_{\delta_f}(\delta_f, Z_f) &= \delta_f^3 - \frac{1}{Z_f+1}\left(2 + \widetilde{m}_2^f - \widetilde{m}_1^f + (1 + 2(\widetilde{m}_2^f - \widetilde{m}_1^f))Z_f\right)\delta_f^2 \\ &+ \frac{1}{Z_f+1}\left(Z_f(\widetilde{m}_2^f - \widetilde{m}_1^f)(2 + \widetilde{m}_2^f - \widetilde{m}_1^f) + (1 + \widetilde{m}_2^f)(1 - \widetilde{m}_1^f)\right)\delta_f \\ &- \frac{Z_f(\widetilde{m}_2^f - \widetilde{m}_1^f)^2}{Z_f+1} = 0. \end{aligned} \tag{43}$$

The equation $(Z_f + 1)F_{\delta_f}(\delta_f, Z_f) = 0$ is a linear function in Z_f, hence given δ_f there is only one solution for Z_f. The χ^2 fits that we performed fitted the parameters δ_f, hence fixing unequivocally the values of Z_f. Had we chosen to fit Z_f, we would have obtained three possible solutions for δ_f. We find that if $Z = O(10)$, the three solutions for δ_f are roughly O(10^{-4}), O(10^{-2}) and O(1), both for $f = u$ and for $f = d$. In Fig. 7 we have plotted one of the solutions, that is close to O(10^{-4}), to $F_{\delta_f}(\delta_f, Z_f) = 0$, for two sets of data, that of 1999 [16] and the analogous solution for the case I of this study, when ϕ_1 is fixed to $\pi/2$. However, for this last set of data, we have used only the best fit points of the parameters $\widetilde{m}_i$ in Tab. 8, but not the value of δ_f. Instead, once the parameters $\widetilde{m}_i$ are fixed, $\delta_f(Z_f)$ is computed as the solution of

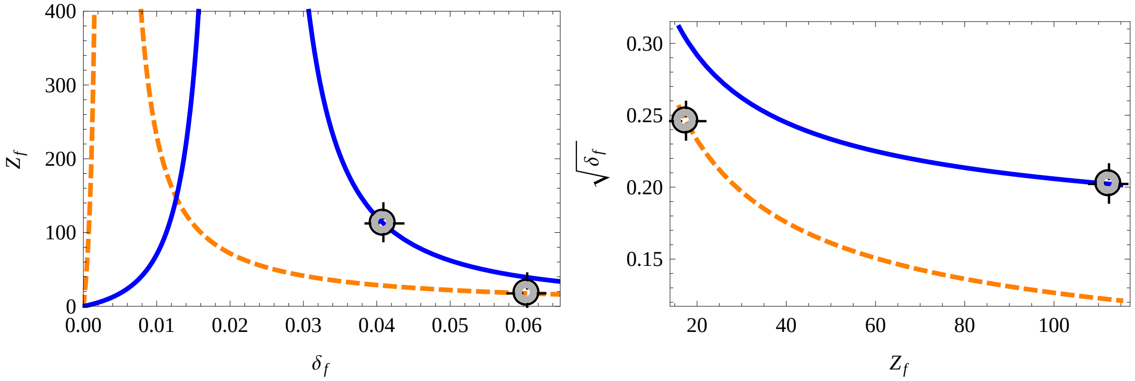

Figure 8: On the left, Z_f as a function of δ_f, $f = u$ blue (solid) curve, $f = d$, orange (dashed) curve. The values obtained, from the fit for the case of $\phi_1 = \pi/2$, for δ_u and δ_d, 0.0605 and 0.0409 fix respectively particular values of Z_f, 112.33 and 17.52. On the left, the parameter $\sqrt{\delta_f}$ as a function of Z_f, $f = u$ blue (solid) curve, $f = d$, orange (dashed) curve, for the data of 2012 for $\phi_1 = \pi/2$, corresponding to another solution of Eq. (43), different from that of Fig. 7. We have marked the points $(17.52, \sqrt{0.049})$ and $(112.33, \sqrt{0.0605})$. We can see that they correspond exactly to the solution of Eq. (43), which is plotted here, since they lie along the line of $F(\delta_f, Z_f) = 0$, and not to the solution of Fig. 7.

Eq. (43) that vanishes when Z_f vanishes. In the first plot of Fig. 8, we show Z_f as function of δ_f, computed from Eq. (43) for values of δ_f close to the values obtained from the fit for case I with ϕ_1 fixed at $\pi/2$. The second plot in Fig. 8 shows $\sqrt{\delta_f}$ as a function of Z_f. In these graphs $\delta_f(Z_f)$ was chosen as the solution of $F_{\delta_f}(\delta_f, Z_f) = 0$ of $\mathrm{O}(10^{-2})$, in this way we check that it is indeed this solution the one determined in the χ^2 fit.

In refs. [16, 17, 22, 51, 66] the solution to Eq. (43) was chosen such that δ_f could represent a parameter of the breaking of S_3, which would vanish in the limit of vanishing Z_f. In the limit $Z_f \to 0$, Eq. (43) has two other solutions for δ_f

$$\delta_f = 1 + \tilde{m}_2^f \quad \text{and} \quad \delta_f = 1 - \tilde{m}_1^f. \tag{44}$$

Notice that neither of them satisfies the inequality $1 - \tilde{m}_1^f > \delta_f > 0$ [51].

7.3.2 Cases II and III (three and four Higgs fields, respectively)

In the cases of three and four Higgs fields, the functional form of the elements of the CKM matrix expressed as functions of the quark masses and the parameters $\tilde{\mu}_0^f$, δ_u, and δ_d is the same. The only difference between the subcases A' and B' for the extended model with three Higgs fields (see Table 4) and among the subcases A', B', C', and D' for the extended model with four Higgs fields (see Table 5) is in the interpretation of the meaning of the parameters that occur as arguments in the elements of the CKM matrix in Eq. (37), which corresponds to taking Eq. (38) with $\phi_1 = 0$ and $\widetilde{\sigma}_i^f = \widetilde{m}_i^f + \tilde{\mu}_0^f$ for $\tilde{\mu}_0^f \neq 0$. Thus, for this case, the relevant parameters to fit are $\tilde{\sigma}_i^f$, $i = 1, 2, 3$, δ_u, δ_d, and ϕ_2, which we denote as p_i. Since the parameters

$\tilde{\sigma}_i^f$ are linear combinations of the mass ratios $\tilde{m}_i^f$ and the parameters $\tilde{\mu}_0^f$, we cannot fit $\tilde{\mu}_0^f$ as part of the minimisation procedure, because then the fit would be underdetermined due to the linear dependence among its parameters. However, in order to give an interpretation to the parameters $\tilde{\mu}_0^f$, one possibility (i), is to let the parameters $\tilde{\sigma}_i^f$ to vary in the region

$$\tilde{m}_i^f - 3\tilde{\sigma}_{\tilde{m}_i^f} \leq \tilde{\sigma}_i^f \leq \tilde{m}_i^f + 3\sigma_{\tilde{m}_i^f} \ , \tag{45}$$

and then check the compatibility of calculating $\tilde{\mu}_0^u$ such that

$$\tilde{\mu}_0^u = \tilde{\sigma}^u - \widetilde{m}_u, \ \rightarrow \ \widetilde{m}_c = \tilde{\sigma}^c - \mu_0^u, \tag{46}$$

where $\widetilde{m}_u$, in the first expression of Eq. (46), should lie within its experimental 3σ region. An analogous procedure is performed for the down-type quark sector. The values of $\tilde{\sigma}^u$ and $\tilde{\sigma}^d$ should correspond to the BFPs of the fit. Another possibility, (ii), is to fit the parameters p_i, for a given value of $\tilde{\mu}_0^f \neq 0$, such that

$$\tilde{m}_i - 3\sigma_{\tilde{m}_i} + \tilde{\mu}_0^f \leq \tilde{\sigma}_u \leq \tilde{m}_i + 3\sigma_{\tilde{m}_i} + \tilde{\mu}_0^f, \tag{47}$$

with $f = u$ for the up-type quarks and $f = d$ for the down-type quarks. Note that the difference in the interpretations of $\tilde{\mu}_0^f$ for the cases above, Eqs.(46,47) lies in the fact that for the case (i) there is no assumption on the value of $\tilde{\mu}_0^f$, but then $\tilde{\mu}_0^u$ necessarily has to be less than $6\sigma_{\widetilde{m}_u}$, while $\tilde{\mu}_0^d$ has necessarily to be less than $6\sigma_{\widetilde{m}_d}$. On the other hand, for (ii), in principle, there is no restriction on the value of the given $\tilde{\mu}_0^f$ parameters. Although δ_u and δ_d have also a linear dependence on $\tilde{\mu}_0^f$, Eq. (31), since the definition involves another free parameter D^f, we can leave δ_u and δ_d to vary as completely free parameters. We performed two sets of fits, one using the 2012 values of the parameters $\widetilde{m}_i$ of Tab. 6 and the other the values of Tab. 7, corresponding to the 2012 values of $\widetilde{m}_i$ when considering only the theoretical determination of $\widetilde{m}_s$. We have allowed $\cos\phi_2$ to vary in the region $(0, 1)$ and, we remind the reader that for this case the phase ϕ_1, in Eq. (38), is equal to 0. The results of this fit are shown in Figs. 9 and 10.

In case (i), we can then calculate the value of $\tilde{\mu}_0^u$ from the experimental central value of $\widetilde{m}_u$, for which we have then $\tilde{\mu}_0^u = -6 \times 10^{-6}$ and consequently, from Eq. (46), $\widetilde{m}_c = 3.942 \times 10^{-3}$, where we have used the values of $\widetilde{\sigma}_u$ quoted in Tab. 9. Analogously for the d sector, we have $\tilde{\mu}_0^d = \tilde{\sigma}_d - \widetilde{m}_d = 3.8 \times 10^{-3}$, as a consequence $\widetilde{m}_s = 2.04 \times 10^{-3}$. Since we have the hierarchies $\widetilde{m}_u << \widetilde{m}_c$ and $\widetilde{m}_d << \widetilde{m}_s$, while non-zero values of $\tilde{\mu}_0^u$ and $\tilde{\mu}_0^d$ may be needed in this model to attain a best value of $\widetilde{m}_u$ and $\widetilde{m}_d$, respectively, concerning $\widetilde{m}_c$ and $\widetilde{m}_s$, the impact is minimal.

8 Conclusions

We have studied the quark sector of different S_3 models, either with one, three or four Higgs electroweak doublets. We presented the most general S_3-invariant Yukawa Lagrangian, which can describe these models. The structure of the Lagrangian gives rise to fermion mass matrices

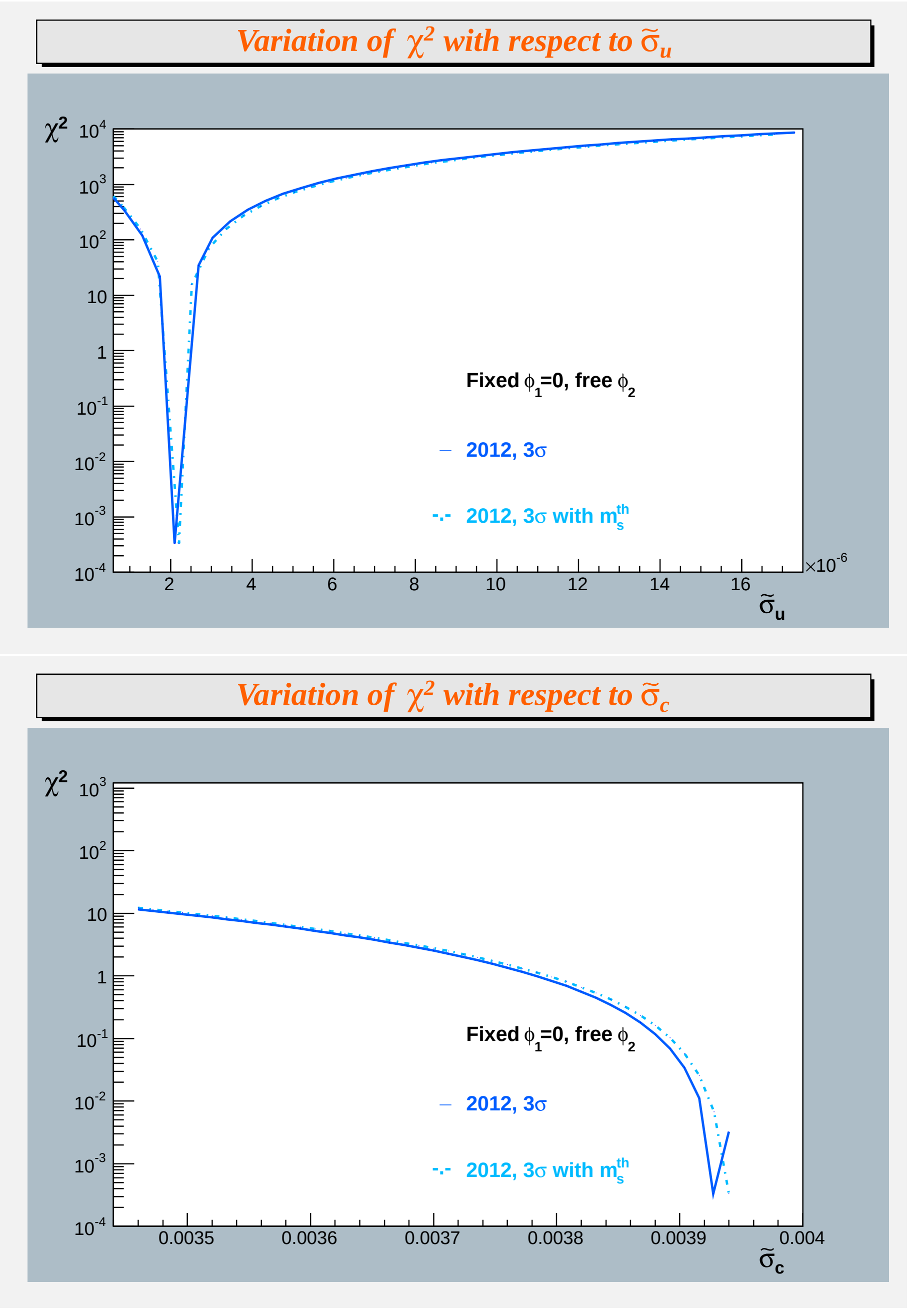

Figure 9: χ^2 as a function of $\tilde{\sigma}_u$ and $\tilde{\sigma}_c$, where $\cos\phi_1$ is allowed to vary in the region $(0.5, 1.0)$. The rest of the details are like those of Fig. 1

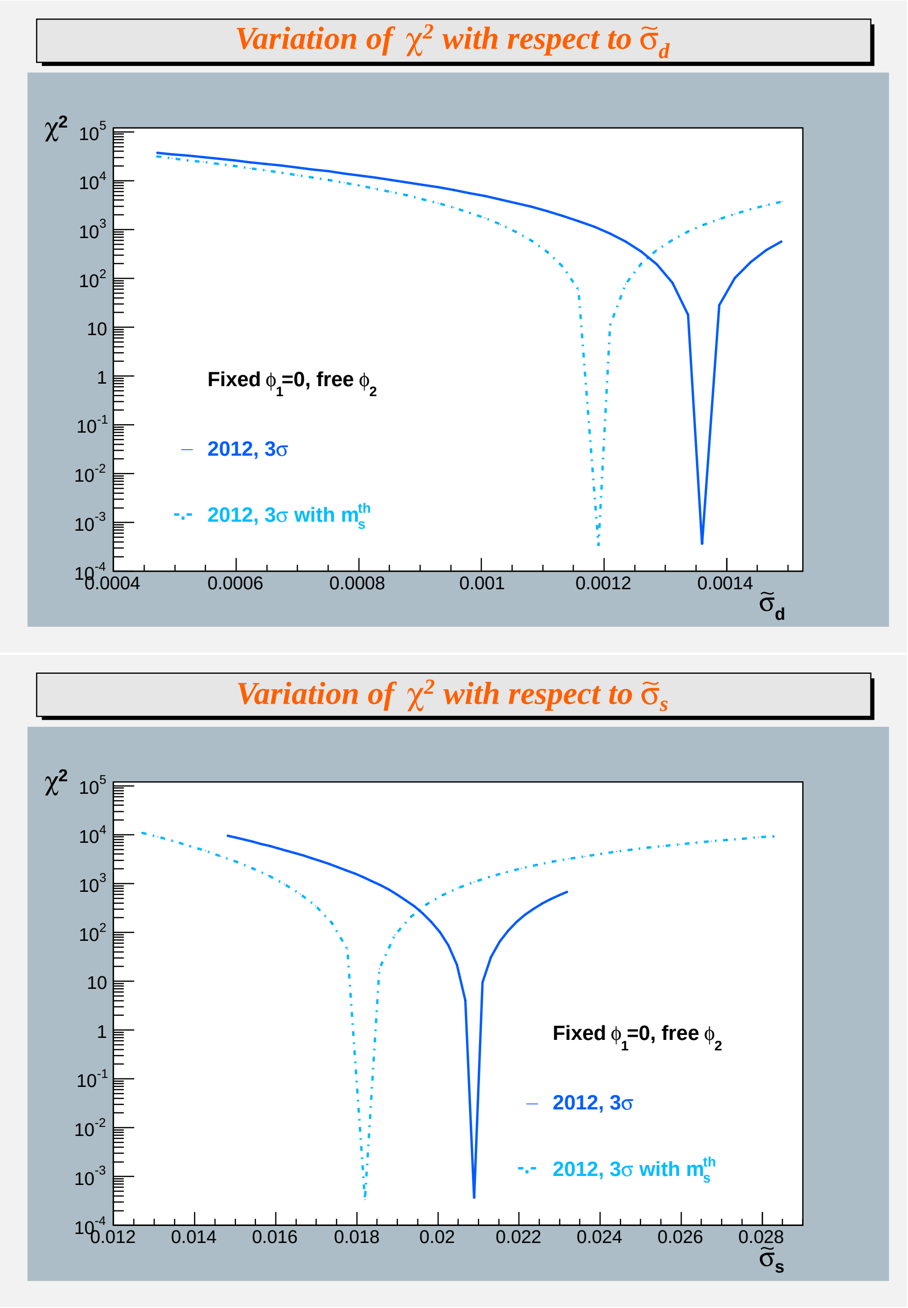

Figure 10: χ^2 as a function of $\widetilde{\sigma}_d$ and $\widetilde{\sigma}_s$, where $\cos\phi_1$ is allowed to vary in the region $(0.5, 1.0)$. The rest of the details are like those of Fig. 1.

Parameter	Central value	χ^2	Values with restricted precision	χ^2
Fit using the 2012 values of the parameters $\widetilde{m}_i$				
$\widetilde{\sigma_u}\,(M_Z)$	2.08977×10^{-6}		$(2.09 \pm 0.19) \times 10^{-6}$	
$\widetilde{\sigma}_c\,(M_Z)$	3.93180×10^{-3}		$(3.93 \pm 0.007) \times 10^{-3}$	
$\widetilde{\sigma}_d\,(M_Z)$	1.35949×10^{-3}		$(1.36 \pm 0.004) \times 10^{-3}$	
$\widetilde{\sigma}_s\,(M_Z)$	2.08443×10^{-2}		$(2.08 \pm 0.02) \times 10^{-2}$	
δ_u	3.96726×10^{-2}		$(3.97 \pm 0.35) \times 10^{-2}$	
δ_d	5.29260×10^{-2}		$(5.29 \pm 041) \times 10^{-2}$	
$\cos\phi_2$	8.48776×10^{-1}		$(8.49 \pm 0.22) \times 10^{-1}$	
		3.3×10^{-4}		3.9×10^{-1}
Fit using the 2012 values of the parameters $\widetilde{m}_i$ (with $\widetilde{m}_s^{th}$)				
$\widetilde{\sigma_u}\,(M_Z)$	2.17737×10^{-6}		$(2.18 \pm 0.35) \times 10^{-6}$	
$\widetilde{\sigma}_c\,(M_Z)$	3.94×10^{-3}		$(3.94 \pm 0.007) \times 10^{-3}$	
$\widetilde{\sigma}_d\,(M_Z)$	1.19392×10^{-3}		$(1.19 \pm 0.009) \times 10^{-3}$	
$\widetilde{\sigma}_s\,(M_Z)$	1.82432×10^{-2}		$(1.82 \pm 0.02) \times 10^{-3}$	
δ_u	6.12747×10^{-2}		$(6.13 \pm 0.41) \times 10^{-2}$	
δ_d	8.36979×10^{-2}		$(8.37 \pm 0.64 \times 10^{-2}$	
$\cos\phi_2$	9.23028×10^{-1}		$(9.23 \pm 0.11) \times 10^{-1}$	
		3.3×10^{-4}		7.3×10^{-2}

Table 9: Results of the fits for Cases II and III, that is the case of an SM invariant under an unbroken S_3 symmetry. Note that when we restrict the precision of the fitted values, we observe a significant change in the value of χ^2.

of a generic form with a small number of free parameters, from which we were able to identify the conditions under which the two texture zeroes and Nearest Neighbour Interaction (NNI) mass matrices are obtained. In all cases we have provided exact, analytical formulas for the mixing angles of the CKM matrix in terms of quark mass ratios and a shift parameter μ_0^f. This line of work had been already developed in ref. [22, 73], without referring to a particular model, where it was shown the usefulness of classifying mass matrix patterns according to their transformation properties under the group of permutations of three objects, S_3. There, it was also shown that a large class of phenomenologically succesful mass matrix forms are equivalent to two texture zeroes matrices. The reduction to these forms, two texture zeroes and NNI, and the fact that all CKM elements can be expressed as analytical relations in terms of quark mass ratios, allowed us to make a direct comparison of the models with the current experimental data. To this end, we performed a χ^2 fit of our theoretical expressions for the CKM mixing matrix to the experimentally determined values of the CKM matrix elements.

In the case of the S_3 model with one Higgs electroweak doublet, which we have called S_3-SM, the S_3 symmetry has to be broken in order to give masses to all fermions. The resulting mass matrix, in a symmetry adapted basis, corresponds to a two zeroes texture. The value of χ^2 of the fit to the CKM elements, is 1.6×10^{-1}. In the case with three (S_3-3H) or four Higgs electroweak doublets the flavour symmetry is preserved. In these cases the resulting mass matrices correspond to either two zeroes textures or NNI ones, both known to be in good agreement with the phenomenology. The functional form of the CKM matrix elements is the same either with three or four Higgses, and the value of χ^2 is 3.9×10^{-1}.

It is worth noting that over the last decade there has been remarkable progress in reducing the uncertainties in the measurement of quark masses. Unlike one decade ago, presently it is no longer good enough to have a model that reproduces the hierarchy of fermion masses within the order of magnitude. At present, there are stringent limits on their values and so one must use statistical methods, such as a χ^2 fit, to measure the validity of a given model to reproduce the observed values for the CKM elements and the quark masses. The results of our χ^2 fits, show that the S_3 models presented here reproduce with a remarkable accuracy the values of the CKM elements. The very good agreement between the S_3 flavour symmetry models of quarks (presented in this work) and leptons [22, 51] mixing, and the experimentally determined values of the corresponding mixing matrices, V^{exp}_{CKM} and V^{exp}_{PMNS}, gives a strong support to the idea that fermion masses and mixing might be related by a flavour permutational symmetry S_3.

Acknowledgements

We thank J. Erler for useful discussions regarding the lattice determinations of m_s. This work was partially supported by DGAPA-UNAM under contract PAPIIT-IN113712-3 and by CONACyT-Mexico under contract No. 132059. F. González Canales acknowledges the financial support received from PROMEP through a postdoctoral scholarship under contract /103.5/12/2548. L. Velasco-Sevilla work was partially supported by an SFB 676 Fellowship at the University of Hamburg, she also acknowledges the attentive hospitality of the IF-UNAM Department of Theoretical Physics.

A Details of the rotation of mass matrices

As we have mentioned in the main body of the text, the matrix $\mathcal{M}^f_{S_3}$ makes explicit the S_3 transformations, however in order to diagonalise the mass matrix and extract the mixing matrix we perform a rotation and a shift as follows

$$\mathcal{M}^f_{Hier} \equiv \mathcal{R}(\theta)_{f12} \mathcal{M}^f_{S_3} \mathcal{R}(\theta)^T_{f12}, \tag{48}$$

where $\mathcal{M}^f_{Hier}$, for sub-cases A and A' of case III, it is explicitly given as

$$\mathcal{M}^f_{Hier} \equiv \begin{pmatrix} \mu^f_1 + \mu^f_2 c^2(1-3t^2) & \mu^f_2 sc(3-t^2) + \mu^f_5 & 0 \\ \mu^f_2 sc(3-t^2) - \mu^f_5 & \mu^f_1 - \mu^f_2 c^2(1-3t^2) & \mu^f_7/c \\ 0 & \mu^f_9/c & \mu^f_3 \end{pmatrix}, \tag{49}$$

while for the B and B' sub-cases of case III is given by

$$\mathcal{M}^f_{Hier} \equiv \begin{pmatrix} \mu^f_1 - \mu^f_4 sc(3-t^2) & -\mu^f_4 c^2(1-3t^2) + \mu^f_5 & 0 \\ -\mu^f_4 c^2(1-3t^2) - \mu^f_5 & \mu^f_1 + \mu^f_4 sc(3-t^2) & -\mu^f_6/c \\ 0 & \mu^f_8/c & \mu^f_3 \end{pmatrix} , \tag{50}$$

where $c = \cos\theta$, $s = \sin\theta$, and $t = \tan\theta$. For sub-cases A, A', B, and B' of case II we just need to set $\mu_5 = 0$. Following Eq. (16) we can then identify that the condition for $(1,3)$ and $(3,1)$ to vanish is

$$\tan\theta = w_1/w_2 \tag{51}$$

or

$$\tan\theta = -w_2/w_1 \tag{52}$$

for sub-cases A and A' or B and B', respectively.

The rotation in the Dirac fermion sector is unobservable, as long as we rotate both matrices, in the u and d or in the l and ν_l sectors, by the same angle θ. Concerning the quark sector, the latter statement can be easily verified by diagonalising the matrices $\mathcal{M}^f_{S_3}$ and the rotated matrices $\mathcal{R}(\theta)_{f12}\ \mathcal{M}^f_{S_3}\mathcal{R}(\theta)^T_{f12}$,

$$\mathcal{M}^f_{\text{diag.}} \; = \; V^f_L \mathcal{M}^f_{S_3} V^{f\dagger}_R, = V^f_L \mathcal{R}(\theta)^T_{f12} \left[\mathcal{R}(\theta)_{f12}\mathcal{M}^f_{S_3}\mathcal{R}(\theta)^T_{f12}\right] \mathcal{R}(\theta)_{f12} V^{f\dagger}_R. \tag{53}$$

It is then readily seen that the physical observables, contained in the CKM matrix, remain invariant

$$V_{\text{CKM}} = V^u_L \mathcal{R}(\theta)^T_{u12}\mathcal{R}(\theta)_{d12} V^{d\dagger}_L. \tag{54}$$

Therefore, as long as we have the same rotation in both sectors, we preserve the matrix structure of the S_3 symmetry. Now, we make a shift such that

$$\mathcal{M}^f_{Hier} = \mu^f_0 \mathbf{1}_{3\times 3} + \widehat{\mathcal{M}^f}_{Hier}, \tag{55}$$

where $\widehat{\mathcal{M}^f}_{Hier}$ has the form of Eq. (23) and hence we can proceed like in ref. [22] to diagonalise the mass matrix, which is explained in this work in Section 5.3. The matrix of Eq. (49) can be identified with that of Eq. (26) by assuming that

$$Y^f_4 = i|Y^f_4|, \quad Y^f_6 = Y^{f*}_5, \tag{56}$$

where the first condition is needed such that the entries $(1,2)$ and $(2,1)$ correspond respectively to the complex conjugate of each other, and the second, such that the entries $(2,3)$ and $(3,2)$

are also complex conjugate of each other. From Eqs. (26) and (49) we can see that the phase ϕ_{1f} is fixed by

$$\tan\phi_{1f} = \frac{|\mu_5|}{\mu_2^f sc(3-t^2)} = \frac{\sqrt{2}|Y_4^f|v_A}{|Y_3^f|w_2 sc(3-t^2)}, \tag{57}$$

or

$$\tan\phi_{1f} = \frac{|\mu_5|}{-\mu_4^f c^2(1-3t^2)} = -\frac{\sqrt{2}|Y_4^f|v_A}{|Y_3^f|w_1 c^2(1-3t^2)}, \tag{58}$$

for sub-cases A and A' or B and B', respectively, which can be written in terms of the invariants of the matrix $\widehat{\mathcal{M}}_{Hier}$ and the free parameter δ^f, which is the form we present in Eq. (35).

For sub-cases A' and B' of cases II and III, Tabs. (1) and (4), respectively, the form of the matrix can be reproduced just by assuming a rotation angle of $\theta = \pi/6$ or $\theta = \pi/3$ for sub-case A' or B', respectively, and without any necessity of imposing Hermiticity to the mass matrix.

References

[1] H. Fritzsch and Z.-z. Xing, Prog.Part.Nucl.Phys. **45**, 1 (2000), arXiv:hep-ph/9912358.

[2] L. Velasco-Sevilla, J.Phys.Conf.Ser. **287**, 012009 (2011).

[3] M. Gupta and G. Ahuja, Int.J.Mod.Phys. **A26**, 2973 (2011).

[4] H. Ishimori *et al.*, Prog.Theor.Phys.Suppl. **183**, 1 (2010), arXiv:1003.3552.

[5] G. Altarelli and F. Feruglio, Rev.Mod.Phys. **82**, 2701 (2010), arXiv:1002.0211.

[6] M. Hirsch *et al.*, (2012), arXiv:1201.5525.

[7] R. Gatto, G. Sartori, and M. Tonin, Phys.Lett. **B28**, 128 (1968).

[8] N. Cabibbo and L. Maiani, Phys.Lett. **B28**, 131 (1968).

[9] H. Pagels, Phys.Rev. **D11**, 1213 (1975).

[10] S. Weinberg, Trans.New York Acad.Sci. **38**, 185 (1977).

[11] F. Wilczek and A. Zee, Phys.Lett. **B70**, 418 (1977).

[12] H. Fritzsch, Phys.Lett. **B70**, 436 (1977).

[13] A. Ebrahim, Phys.Lett. **B73**, 181 (1978).

[14] R. N. Mohapatra and G. Senjanovic, Phys.Lett. **B73**, 176 (1978).

[15] H. Fritzsch, Phys.Lett. **B73**, 317 (1978).

[16] A. Mondragón and E. Rodríguez-Jáuregui, Phys.Rev. **D59**, 093009 (1999), arXiv:hep-ph/9807214.

[17] A. Mondragón and E. Rodríguez-Jáuregui, Phys.Rev. **D61**, 113002 (2000), arXiv:hep-ph/9906429.

[18] S. Morisi, (2006), arXiv:hep-ph/0604106.

[19] F. Feruglio and Y. Lin, Nucl.Phys. **B800**, 77 (2008), arXiv:0712.1528.

[20] T. Kobayashi, Y. Omura, and K. Yoshioka, Phys.Rev. **D78**, 115006 (2008), arXiv:0809.3064.

[21] R. Jora, J. Schechter, and M. Naeem Shahid, Phys.Rev. **D80**, 093007 (2009), arXiv:0909.4414.

[22] J. Barranco, F. González Canales, and A. Mondragón, Phys.Rev. **D82**, 073010 (2010), arXiv:1004.3781.

[23] Z.-z. Xing, D. Yang, and S. Zhou, Phys.Lett. **B690**, 304 (2010), arXiv:1004.4234.

[24] S. Zhou, Phys.Lett. **B704**, 291 (2011), arXiv:1106.4808.

[25] D. Meloni, JHEP **1205**, 124 (2012), arXiv:1203.3126.

[26] S. Dev, R. R. Gautam, and L. Singh, Phys.Lett. **B708**, 284 (2012), arXiv:1201.3755.

[27] H. Benaoum, (2013), arXiv:1302.0950.

[28] S. Pakvasa and H. Sugawara, Phys.Lett. **B73**, 61 (1978).

[29] E. Derman, Phys.Rev. **D19**, 317 (1979).

[30] D. Wyler, Phys.Rev. **D19**, 330 (1979).

[31] J.-M. Frere, Phys.Lett. **B80**, 369 (1979).

[32] R. Yahalom, Phys.Rev. **D29**, 536 (1984).

[33] E. Ma, Phys.Rev. **D43**, 2761 (1991).

[34] L. J. Hall and H. Murayama, Phys.Rev.Lett. **75**, 3985 (1995), arXiv:hep-ph/9508296.

[35] L. Lavoura, Phys.Rev. **D61**, 077303 (2000), arXiv:hep-ph/9907538.

[36] Y. Koide, Phys.Rev. **D60**, 077301 (1999), arXiv:hep-ph/9905416, Revised version.

[37] J. Kubo, A. Mondragón, M. Mondragón, and E. Rodríguez-Jáuregui, Prog.Theor.Phys. **109**, 795 (2003), arXiv:hep-ph/0302196.

[38] J. Kubo, H. Okada, and F. Sakamaki, Phys.Rev. **D70**, 036007 (2004), arXiv:hep-ph/0402089.

[39] S.-L. Chen, M. Frigerio, and E. Ma, Phys.Rev. **D70**, 073008 (2004), arXiv:hep-ph/0404084.

[40] Y. Koide, Phys.Rev. **D73**, 057901 (2006), arXiv:hep-ph/0509214.

[41] T. Kimura, Prog.Theor.Phys. **114**, 329 (2005).

[42] T. Araki, J. Kubo, and E. A. Paschos, Eur.Phys.J. **C45**, 465 (2006), arXiv:hep-ph/0502164.

[43] A. Mondragón, M. Mondragón, and E. Peinado, J.Phys. **A41**, 304035 (2008), arXiv:0712.1799.

[44] S. Kaneko, H. Sawanaka, T. Shingai, M. Tanimoto, and K. Yoshioka, (2007), arXiv:hep-ph/0703250.

[45] A. Mondragón, M. Mondragón, and E. Peinado, AIP Conf.Proc. **1026**, 164 (2008), arXiv:0712.2488.

[46] A. Mondragón, M. Mondragón, and E. Peinado, Phys.Rev. **D76**, 076003 (2007), arXiv:0706.0354.

[47] O. F. Beltrán, M. Mondragón, and E. Rodríguez-Jáuregui, J.Phys.Conf.Ser. **171**, 012028 (2009).

[48] G. Bhattacharyya, P. Leser, and H. Pas, Phys.Rev. **D83**, 011701 (2011), arXiv:1006.5597.

[49] T. Teshima and Y. Okumura, Phys.Rev. **D84**, 016003 (2011), arXiv:1103.6127.

[50] T. Teshima, Phys.Rev. **D85**, 105013 (2012), arXiv:1202.4528.

[51] F. González Canales, A. Mondragón, and M. Mondragón, Fortschritte der **Physik** (2012), arXiv:1205.4755.

[52] Particle Data Group, J. Beringer *et al.*, Phys. Rev. **D86**, 010001 (2012).

[53] G. Fogli *et al.*, Phys.Rev. **D86**, 013012 (2012), arXiv:1205.5254.

[54] D. Forero, M. Tortola, and J. Valle, Phys.Rev. **D86**, 073012 (2012), arXiv:1205.4018.

[55] Particle Data Group, K. Nakamura *et al.*, J.Phys.G **G37**, 075021 (2010).

[56] A. Mondragón *et al.*, Work in progress.

[57] J. Girrbach, p. 83 (2012), arXiv:1208.5630.

[58] S. F. King and C. Luhn, (2013), arXiv:1301.1340.

[59] D. Emmanuel-Costa, C. Simoes, and M. Tortola, (2013), arXiv:1303.5699.

[60] J. Gómez-Izquierdo, F. González Canales, and M. Mondragón, A Grand Unified Model with Q6 as the Flavour Symmetry. To appear in the proceedings of PASCOS 2012.

[61] CMS Collaboration, S. Chatrchyan *et al.*, (2013), arXiv:1302.1764.

[62] N. Haba and K. Yoshioka, Nucl.Phys. **B739**, 254 (2006), arXiv:hep-ph/0511108.

[63] ATLAS Collaboration, G. Aad *et al.*, Phys.Lett. **B716**, 1 (2012), arXiv:1207.7214.

[64] CMS Collaboration, S. Chatrchyan *et al.*, Phys.Lett. **B716**, 30 (2012), arXiv:1207.7235.

[65] CMS Collaboration, S. Chatrchyan *et al.*, (2013), arXiv:1303.4571.

[66] A. Mondragón and E. Rodríguez-Jáuregui, Rev.Mex.Fis. **46**, 5 (2000), arXiv:hep-ph/0003104.

[67] K. Harayama and N. Okamura, Phys.Lett. **B387**, 614 (1996), arXiv:hep-ph/9605215.

[68] K. Harayama, N. Okamura, A. Sanda, and Z.-Z. Xing, Prog.Theor.Phys. **97**, 781 (1997), arXiv:hep-ph/9607461.

[69] F. González-Canales, A. Mondragón, U. Saldaña Salazar, and L. Velasco-Sevilla, (2012), arXiv:1210.0288.

[70] K. Chetyrkin, J. H. Kuhn, and M. Steinhauser, Comput.Phys.Commun. **133**, 43 (2000), arXiv:hep-ph/0004189.

[71] Z.-z. Xing, H. Zhang, and S. Zhou, Phys.Rev. **D77**, 113016 (2008), arXiv:0712.1419.

[72] R. Brun and F. Rademakers, Proceedings AIHENP'96 Workshop, Lausanne, Sep. 1996, Nucl. Inst. & Meth. in Phys. Res. A , 81 (389 (1997)).

[73] F. González Canales and A. Mondragón, J.Phys.Conf.Ser. **287**, 012015 (2011), arXiv:1101.3807, Presented at XIV Mexican School on Particles and Fields, 4-13 November 2010, Morelia México.